TAMPEREEN TEKNILLINEN YLIOPISTO
TAMPERE UNIVERSITY OF TECHNOLOGY

TOPI NISKALA

USING GRAPHENE OXIDE AS A COMPATIBILIZER IN IMMISCIBLE POLYMER BLENDS

Master of Science Thesis

Examiners: Asst. Prof. Essi Sarlin, Postdoctoral Researcher Rama Layek, University Teacher Ilari Jönkkäri
Examiners and topic approved by the Faculty Council of the Faculty of Engineering Sciences on 29th of August 2018

ABSTRACT

TOPI NISKALA: Using graphene oxide as a compatibilizer in immiscible polymer blends
Tampere University of Technology
Master of Science Thesis, 55 pages
September 2018
Master's Degree Programme in Materials Science
Major: Polymers and Biomaterials
Examiners: Assistant Professor Essi Sarlin, Postdoctoral Researcher Rama Layek and University Teacher Ilari Jönkkäri.

Keywords: Low-density polyethylene, polyamide 66, graphene oxide, polymer blend, compatibilization, dispersion, miscibility

In this thesis, normally highly immiscible blends of low-density polyethylene and polyamide 66 were created and studied. Blends, which are based on engineering thermoplastic, like polyamide, and on commodity plastic, like polyethylene, are an interesting research target because it would be possible to create blends, with many desired properties and low cost. These blends could be then exploited in many applications in different fields. The usual problem of polymer blending is related to the different chemical structures of blend's components. This leads to phase separation in the blend, which leads to poor properties. To tackle this problem, a third component can be added to the blend. These components are called compatibilizers and they are usually block or graft copolymers but using them in blends has many challenges. That is why in this work, graphene oxide was used as a compatibilizer to research its potential to enhance blends properties.

The theoretical part of the thesis presents information about low-density polyethylene, polyamide66, polymer blending and graphene. The basic properties, structural information and typical uses of low-density polyethylene and polyamide 66 are discussed first. Followed by this, is a section of polymer blending. Polymer blending is introduced by providing information about extruders, mixing processes and thermodynamics. Also, compatibilizers are introduced. Finally, graphene is presented. The focus is mainly on graphene oxide and reduced graphene oxide, providing information about their structures, properties and ways to produce them. The functionalization of graphene oxide is also presented.

The experimental part included modified Hummers' method to produce graphene oxide and preparation of suitable masterbatches for processing. Melt compounding with twin-screw extruder was performed to mix the blends and to potentially partially reduce and functionalize the graphene oxide. Various characterization methods were used in this work with suitable programs to analyze the samples and to see if there were any indications about successful blending.

Several characterization methods indicate, that the dispersion of polyamide 66 in low-density polyethylene matrix was enhanced with the use of partially reduced and non-covalently functionalized graphene oxide as a compatibilizer. This is a key thing in blending and in enhancing blends properties. Also, positive results on enhanced thermal properties and chemical interactions between components are witnessed.

TIIVISTELMÄ

TOPI NISKALA: Sekoittumattoman polymeeriseoksen sekoittuvuuden parantaminen grafeenioksidin avulla
Tampereen teknillinen yliopisto
Diplomityö, 55 sivua
Syyskuu 2018
Materiaalitekniikan diplomi-insinöörin tutkinto-ohjelma
Pääaine: Polymeerit ja Biomateriaalit
Tarkastajat: Assistant Professor Essi Sarlin, Postdoctoral Researcher Rama Layek, University Teacher Ilari Jönkkäri

Avainsanat: pienitiheyksinen polyeteeni, polyamidi 66, grafeenioksidi, polymeeriseos, dispersio, sekoittuvuus

Tämän työn aikana muodostettiin polymeeriseoksia, jotka koostuivat pienitiheyksisestä polyeteenistä ja polyamidi 66:sta. Normaalisti nämä kaksi polymeerilaatua ovat toisiinsa sekoittumattomia, johtuen komponenttien erilaisista kemiallisista rakenteista. Teknisen muovin, kuten polyamidin, ja valtamuovin, kuten polyeteenin, sekoittaminen toisiinsa on mielenkiintoinen tutkimusaihe. Mikäli teknisen muovin ja valtamuovin sekoittaminen toisiinsa onnistuu, syntyy uusia polymeeriseoksia, joilla on hyvät ominaisuudet ja edullinen hinta. Näin ollen näillä polymeeriseoksilla olisi lukuisia eri käyttökohteita eri sovelluksissa. Seosten muodostaminen on kuitenkin hankalaa, johtuen polymeerilaatujen erilaisista kemiallisista rakenteista. Tämä aiheuttaa seosten faasierottumista, mikä puolestaan johtaa huonoihin ominaisuuksiin. Erilaisia sekoittumisen parantamisaineita, kuten kopolymeerejä, on olemassa, mutta niiden käytössä on omat haasteensa. Tämän vuoksi tässä työssä keskitytään tutkimaan grafeenioksidin potentiaalia sekoittuvuuden parantajana ja siten seosten ominaisuuksien parantajana.

Teoriaosuudessa esitellään tietoa pienitiheyksisestä polyeteenistä, polyamidi 66:sta, polymeerien seostamisesta ja grafeenista. Aluksi käydään läpi käytettyjen polymeerien ominaisuudet, rakenteet ja tyypillisimmät käyttökohteet. Tämän jälkeen keskitytään polymeeriseoksiin. Seos-osuudessa käsitellään ekstruudereita, seostusprosesseja ja termodynamiikkaa. Myös sekoittuvuutta parantavia aineita käsitellään tässä osiossa. Lopuksi käydään läpi grafeeniin liittyviä asioita. Grafeeni-osiossa keskitytään grafeenioksidin ja redusoidun grafeenioksidin rakenteisiin, ominaisuuksiin sekä valmistustapoihin. Osio sisältää myös tietoa grafeenioksidin funktionalisoimisesta.

Kokeellinen osa sisälsi modifioidun Hummersin metodin, jota käytetään grafeenioksidin valmistamiseen. Myös sopivien masterbatchien muodostaminen prosessointia varten oli osa kokeellista osiota. Polymeerien prosessointi kaksoisruuvi-ekstruuderissa sekä erilaisten analyysilaitteiden käyttö ja tulosten tulkitseminen olivat myös osa tämän työn kokeellista osiota.

Useat työssä käytetyt analyysilaitteistot osoittavat dispersion parantuneen polymeeriseoksessa, kun seokseen on lisätty grafeenioksidia ja aineet on prosessoitu ekstruuderilla. Dispersion parantuminen on tärkeä asia seosten onnistumisessa ja ominaisuuksien parantamisessa. Myös viitteitä lämpöominaisuuksien parantumisesta ja kemiallisten sidosten olemassaolosta oli havaittavissa.

PREFACE

This Master of Science Thesis was made at Tampere University of Technology's Plastics and Elastomer Technology research group.

I would like to thank Assistant Professor Essi Sarlin, University Teacher Ilari Jönkkäri and Postdoctoral Researcher Rama Layek for the possibility to do this interesting thesis and for all the knowledge, help and feedback that I have received during this project. Also, big thank you to Essi Sarlin for taking the SEM-images, Rama Layek for helping with the FTIR measurements and Alexandra Shakun and Clara Lessa Belone for providing right parameters and measurements in DSC and TGA.

I would also like to thank my family and friends for supporting me during my studies and during this project.

Tampere, 12.9.2018

Topi Niskala

SISÄLLYSLUETTELO

LIST OF SYMBOLS AND ABBREVIATIONS

CVD	Chemical Vapour Deposition
DSC	Differential Scanning Calorimetry
FESEM	Field Emission Scanning Electron Microscope
FTIR	Fourier Transform Infrared spectroscopy
GO	graphene oxide
HDPE	high-density polyethylene
Lcst	lower critical solution temperature
LDPE	low-density polyethylene
LLDPE	linear low-density polyethylene
PA66	polyamide 66
PA6	polyamide 6
PA	polyamide
rGO	reduced graphene oxide
TGA	Thermogravimetric analysis
TUT	Tampere University of Technology
Ucst	upper critical solution temperature
XRD	X-ray Diffraction

d	distance
ΔG_m	free energy
ΔH_m	enthalpy
ΔH_m^0	theoretical enthalpy
K	degree of crystallinity
λ	wavelength
p	pressure
ΔS_m	entropy
T	temperature
θ	diffraction angle
$\emptyset$	composition

1. INTRODUCTION

Polymer blending is an activity, where the goal is to obtain new materials which have desired properties and improved performance with an economical way. Another important aspect of polymer blending is to allow the recycling of the degraded polymeric materials, which is more difficult with laminated or coextruded products [1]. Blending process is typically done by mixer equipment, like twin-screw extruder. Intermeshing co-rotating twin-screw extruders can produce high shear forces and mix different components efficiently [2].

Blends, which have a cheaper commodity polymer component, like polyethylene, and a more expensive engineering polymer component, like polyamide, can provide a wide range of desired properties especially from the point of view of packaging industry. Therefore, they are an interesting target for blend research. However, these polymers are an example of materials, which together form a highly immiscible blend. That is why an efficient compatibilization method would be useful [1,3].

The main problems in polymer blending are usually related to the immiscibility of the blend's different components. Immiscibility is caused by different chemical structures of the blends components, which in most cases leads to poor properties. Miscibility of the blends different components is related to the compatibility of the blend. Typically, polymer blends require the use of compatibilizers, which usually are grafted copolymers or block copolymers. Also, nanomaterials can be exploited in compatibilization. The main object of compatibilizers is to lower the interfacial tension, to stabilize the morphology, to enhance finer dispersion and to improve the phase adhesion. [1,3].

Graphene, and other materials which are based on graphene, have many unique properties. These unique properties have launched the interest for researching graphene in different applications [4]. Graphene oxide can be produced with modified Hummers' method from plentiful graphite. Graphene oxide can also be further reduced and functionalized to exploit its properties in different applications [5].

The main goal of this thesis is to research the blending of low-density polyethylene, polyamide and graphene oxide, to analyze the results and to estimate if partially reduced and functionalized graphene oxide has potential working as a compatibilizer. Focus of this work is mainly on evaluating thermal properties, dispersion and chemical interactions in the blends

The theoretical part of this thesis concentrates on low-density polyethylene's and polyamide's properties and chemical structures. Theoretical part also introduces graphene and other graphenic materials, their properties, structures and ways of producing and exploiting them. Furthermore, polymer blends and mixing of polymers are also discussed in the theory part.

The experimental part focuses on producing of graphene oxide with modified Hummer's method and melt mixing low-density polyethylene, polyamide 66 and graphene oxide with a twin-screw extruder. Several analyzing methods have been used during this thesis to gather information about the blends and to compare the blends with different contents of graphene oxide in them.

2. POLYMERS AND POLYMER BLENDS

2.1 Low-density polyethylene

Polyethylenes are semi-crystalline thermoplastic polymers and a part of a group called polyolefins. The monomer of polyethylene is ethylene (C_2H_4) from which the polyethylenes are processed by polymerization. Polyethylene's are further classified by their density. Low-density polyethylene (LDPE) is one of the most common polyethylene grades together with high-density polyethylene (HDPE) and linear low-density polyethylene (LLDPE) [6].

2.1.1 Properties

Density of LDPE varies in literature between 0.91 – 0.94 g/cm^3 and its melting temperature is approximately 110 – 115 ºC. Structure of LDPE consists of short and long chain branching. Long branches cause irregular packing of molecules which lowers the crystallinity and therefore reduces the density which affects the different properties of the polymer, like thermal and mechanical properties. The degree of crystallinity of LDPE usually vary between 50 – 65% [6,7]. The short and long branching of LDPE is presented in figure 1 [8].

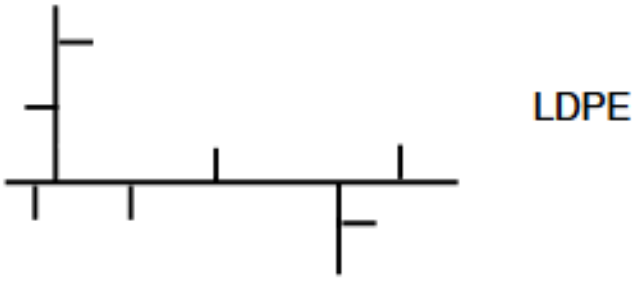

Figure 1. *The typical long and short chain branching of LDPE [8].*

LDPE has many useful properties, which explains its wide use in industry. LDPE is an economical option because it has a low price and it is easy to process using many different methods. LDPE is also an excellent moisture barrier and has good heat sealing properties. LDPE is also relatively chemically inert, taste- and odor-free. Other properties of LDPE include flexibility and transparency. Although LDPE has excellent moisture barrier properties, it also has poor gas barrier properties, especially to CO_2. LDPE has also quite low mechanical strength and heat resistance [6,9].

2.1.2 Processing and applications

LDPE is widely used in industry because of its numerous properties. Because of easy processability, LDPE can be processed with many different methods to make different products. Methods that can be used to produce polyethylene products include: extrusion, thermoforming, blow molding and injection molding, among others [6,10,11].

The biggest amount of LDPE is used for different film applications, mainly by packaging industry for short-term applications [6,10,11]. It is also typical to use polymer blends, where LDPE is one component or to use LDPE in coextrusion or lamination to ensure desired properties [10]. The different film applications are numerous and differ in properties depending on what kind of properties are needed. Typical products include things like bags, liners and bottles, but LDPE can also be used in things like toys and containers. [6,11]. Typical uses of LDPE and LLDPE are illustrated in figure 2 [12].

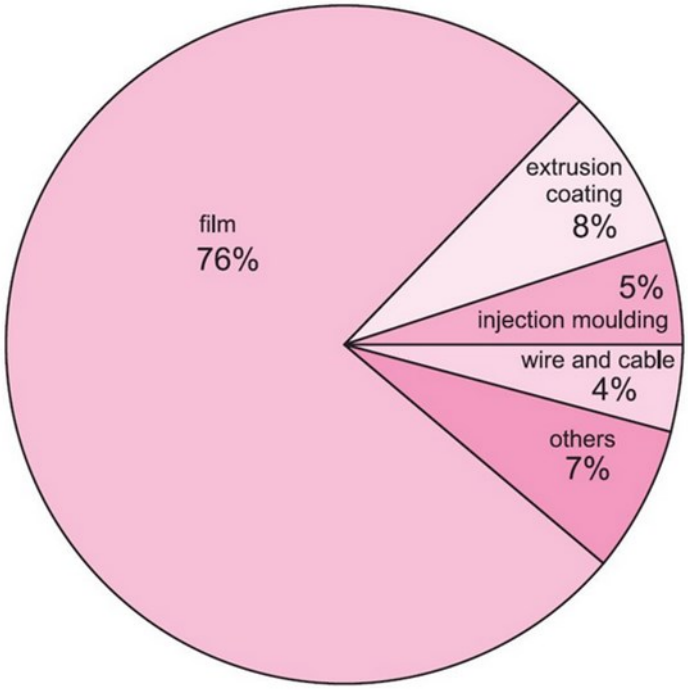

Figure 2. *Most common uses of LDPE & LLDPE [12].*

2.2 Polyamides

Polyamides (PA) are thermoplastic engineering polymers, which are also typically called nylons. Polyamides are mostly linear aliphatic polymers, which contain a repeating amide group (-CONH-) but they can also be aromatic. Many synthetic polyamides are derived from monomers that contain 6-12 carbon atoms [2,13,14].

2.2.1 Properties

Polyamides are engineering polymers which can be divided into aliphatic and aromatic polyamides. Aliphatic polyamides are clearly the most common polyamides. Polyamides can be processed by using many different processing techniques like injection, extrusion, blow molding, rotomolding, coating and others. Polyamides are used in many different applications and products, for example in fibers, automotive industry, packaging industry and electronic applications [2,14,15].

Polyamides can be formed by condensation polymerization from monomers that combine to make amide groups. Another possibility is ring-opening polymerization, which is typically used to form polyamide 6 (PA6). Amide group (-CONH-) is present in every repeating unit of the polymer and is therefore a major determiner of polyamides properties. Amide group's N-H bond and C-O bond are both polar. This induces the formation of secondary bonds between adjacent polyamide molecules. These secondary bonds restrict the movement of the polyamide molecules which increases tensile strength. The secondary bonding also results in high crystallinity polyamide molecules because of the close packing. The high crystallinity leads to characteristics like high strength, good toughness, sharp melting point, good abrasion resistance, high stiffness, low gas and vapor permeability [2,15].

Amide group's polarity also affects the water absorption of polyamide, making it sensitive to polar solvents. The water absorption of polyamide is higher than in most other engineering thermoplastics. Water absorption tendency can have a significant effect on the properties of polyamide, for example decreasing tensile strength and tensile modulus. The water absorption tendency also increases with temperature which is why polyamide should not be exposed to hot water. Absorptivity complicates also the processing of polyamides, because polyamide resins must be dried before processing [2,14].

The sharp melting point of polyamide and the accompanying low viscosity of the melt are advantages in injection molding. On the other hand, they are a disadvantage in processes like extrusion and blow molding which require melt strength [2].

2.2.2 Resins and applications

There are many different types of polyamides and the differences between them largely depend on the number of carbons in the molecular segments between the amide groups. These segments are CH_2 units from the monomers used to form the polyamide. The most common resins of polyamides are PA6 and polyamide 66 (PA66). The monomer of PA6 is caprolactam ($C_6H_{11}NO$) and the monomers of PA66 are hexamethylenediamine ($C_6H_{16}N_2$) and adipic acid ($C_6H_{10}O_4$) [2,14,15]. The most important aliphatic polyamide resins, their monomers and their melting temperatures are presented in table 1. The C-

number in parenthesis refers to the number of carbon atoms in each monomer. As mentioned, this is one important factor to the structure and the properties of the formed polymers.

Table 1. *The most important aliphatic polyamide resins, their monomers and melting temperatures, modified from [13].*

Resin	Monomer(s)	Melting temperature
PA66	Hexamethylenediamine (C6) Adipic acid (C6)	260°C
PA6	Caprolactam (C6)	220°C
PA610	Hexamethylenediamine (C6) Sebacic acid (C10)	220°C
PA612	Hexamethylenediamine (C6) Dodecane diacid (C12)	215°C
PA11	11-aminoundecanoic acid (C11)	185°C
PA12	ω-aminolauric acid (C12) or laurolactam (C12)	178°C

One common way to modify the performance of polyamides is to use fillers like glass fibers, carbon fibers or minerals. Fillers usually provide additional strength or toughness which can be exploited in different applications [2,14,15].

Another polyamide material is a highly aromatic polymer which contains the amide groups with benzene ring between them. These materials are typically called aramids. Aramids have unique properties compared to other polyamides. The high aromatic content has a significant effect on the stiffness and the strength of the material. Bulletproof vests are a good example of a product made by exploiting aramid fibers [2].

2.3 LDPE-PA blends

Polymer blends are designed to create materials which have enhanced properties compared to the individual components of the blend. Blends are researched and created mainly because they offer a cheaper, faster and more environmental-friendly route to create advanced materials, compared to developing new monomers or new polymerization routes. By changing the polymers and by varying the compositions of the selected polymers, the properties of polymer blends can be modified [1,16,17].

The usual problem with creating polymer blends is the unfavorable enthalpy of mixing, which is caused by the different chemical structures of the blend's components. This causes many polymer blends to phase separate. Phase separation is related to the interface of the polymer components, which has a large effect on polymer blend's properties. Phase

separation leads to, for example, poor mechanical properties which is not desirable. That is why it is important to control the phase behavior and the morphology of immiscible polymer blends [1,3,17-19].

Blends which are based on expensive engineering thermoplastics and cheaper commodity plastics play an important role in mixing different polymers. This way it is possible to create blends which have many desired properties at a low cost. It also allows the possibility of recycling wasted raw materials, which is more difficult in coextruded and laminated products [1,20].

In PA and LDPE blends the LDPE component improves, for example, the processability and the PA component improves the resistance to oxygen permeability. This kind of properties are desired by the packaging industry, in application like films. The problem, however, is that LDPE and PA are highly incompatible with each other. This causes the blends to be immiscible and that is why an efficient compatibilizer is needed [1,20].

2.3.1 Thermodynamics of polymer blends

When two polymers are mixed, the mix usually results to a highly immiscible blend due to complete phase separation. This is because of the chemical incompatibility of the two different polymers. Complete miscibility of polymers means that the blend is homogenous down to the molecular level. In a system where there are two polymers, it is required that the following condition, which is also Gibbs free energy of mixing, is met [21-23]:

$$\Delta G_m = \Delta H_m - T\Delta S_m < 0 \quad (1)$$

where, ΔG_m is the free energy of mixing, ΔH_m is the enthalpy of mixing, ΔS_m is the entropy of mixing and T is the absolute temperature.

In a stable one-phase system the requirement for the phase stability of binary mixtures is the following equation [21-23]:

$$\Delta G_m < 0 \quad ,$$

$$\left(\frac{\partial^2 \Delta G_m}{\partial \emptyset_i^2}\right)_{T,p} > 0 \quad (2)$$

where, $\emptyset$ is the composition of the mixture. T is temperature and p is pressure.

Miscible polymer blend is homogenous in the molecular level and it is associated with the negative value of free energy of mixing as can be seen in equations 1 and 2. In miscible polymer blend, the domain size is also comparable to the dimensions of macromolecular statistical segment. Because mixing increases entropy, the value of $T\Delta S_m$ is always positive. That is why the value of ΔG_m depends on the enthalpy of mixing, ΔH_m. That leads to a situation where two polymers mix forming a single phase only when the entropic

contribution to free energy is larger than the enthalpic contribution. For the majority of polymer blends, the miscibility increases with increasing pressure. This happens when $\Delta H_m < 0$, whereas if $\Delta H_m > 0$ the miscibility decreases with increasing pressure [22,24].

A phase diagram is shown in figure 3. It includes the three different degree of miscibility. The single-phase miscible region is located between the two binodals. The binodals and the spinodals border the 4 metastable regions and the spinodals border the two-phase separated regions of immiscibility [22,24].

The diagram also presents the upper critical solution temperatures (Ucst) and the lower critical solution temperatures (Lcst). Diagram with two critical points is a rule for mixtures of components which have low molar mass. Polymer-polymer mixtures generally exhibit Lcst, but also the Ucst is possible [22,24].

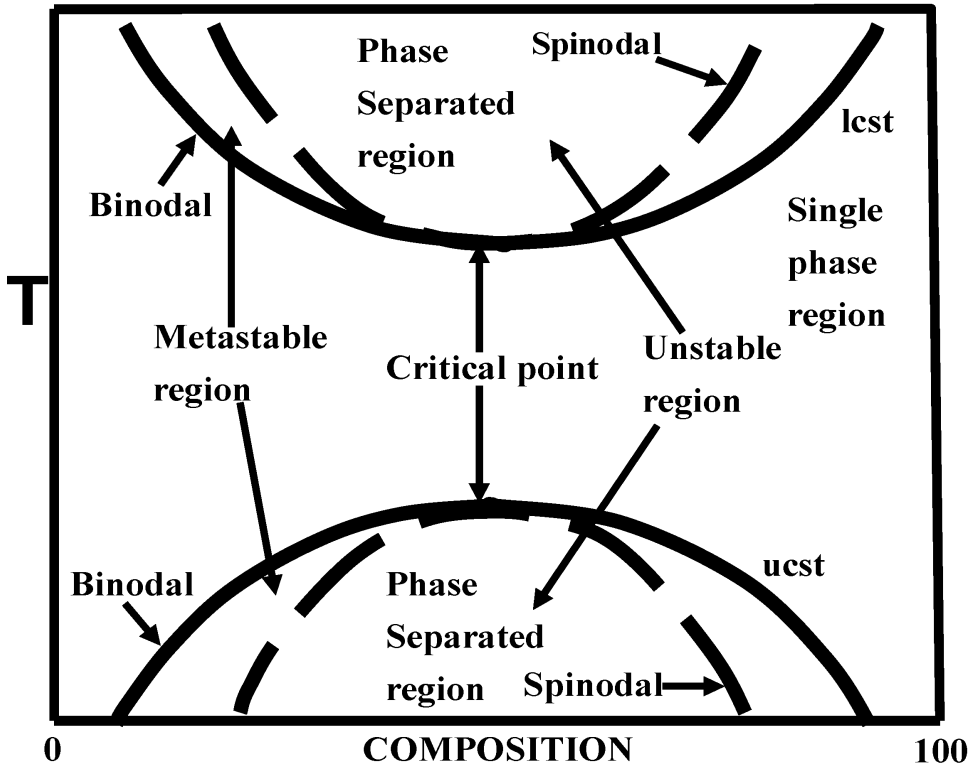

Figure 3. *Phase diagram for liquid mixtures [21].*

When a change of temperature, composition or pressure occurs in a single-phase system, a phase separation may happen. In this case the change forces the single-phase system to enter either the metastable or the spinodal region. The phase separation occurs in a different way depending on whether the system enters from single-phase system to the metastable region or to the spinodal region [22,24].

When the entering happens from single-phase region to the metastable region, the phase separation happens by slow nucleation, which is followed by growth of the phase separated domains. This mechanism resembles crystallization. On the other hand, when the

entering happens from single-phase region to the spinodal region, phase separation happens by spinodal decomposition [21].

2.4 Compatibilizers

Interfacial properties have been traditionally modified by adding a third component, a compatibilizer, to the polymer blend. The most typical compatibilizers are block or graft copolymers, but also nanoparticles, which are compatible with both faces, can have similar effect. The main object of compatibilizers is to lower the interfacial tension, to stabilize the morphology, to enhance finer dispersion and to improve the phase adhesion. Despite this conventional use of block or graft copolymers as compatibilizers has its advantages, they still suffer from certain drawbacks. Copolymers are usually quite specific to certain polymer blends and they are difficult to produce to systems with more than two components. Another drawback of copolymers is that they are expensive to engineer. Due to these drawbacks, finding another economical compatibilization way would be beneficial [1,3,17,25].

3. MIXING OF POLYMERS

3.1 Mixing processes

As the polymer melt is mixed with another immiscible polymer, the polymer melt forms a continuous matrix and the additional polymer becomes a dispersed phase, which forms discrete domains imbedded in the matrix. Blending of polymers requires the different components to be homogeneously mixed with the right proportions. Different processing variables of the extrusion process also have a large influence on the products properties [26].

The mixing process is usually done by a single-screw or a twin-screw extruder, which conveys, melts, meters and mixes the components. Single-screw extruders do not provide enough mixing as such and that is why there are many kinds of designs available for screws, screw elements and barrels depending on the process. Twin-screw extruder, however, is an efficient mixer. Especially the intermeshing corotating twin-screw extruder provides high shear rates to mix the components. Melting occurs mainly caused by the screw rotation, which causes internal frictional heating but also barrel heaters affect the melting [2,27,28].

Mixing is described as dispersive and distributive mixing, which are both required to compound polymers. Dispersive mixing, which is also called intensive mixing, happens when the stress in the melt exceeds the coherent strength of the component. In other words, dispersion is achieved with high shear forces which require high amount of energy. Dispersive mixing reduces the size of any dispersed particles. Distributive mixing means the uniform distribution of the particles in space. Distributive mixing does not require high stress like dispersive mixing. Distributive mixing is achieved because of different velocities of the melt at different locations of the system. In real processes, distributive mixing involves some dispersive mixing and dispersive mixing involves some distributive mixing [26,28]. Dispersive and distributive mixing are illustrated in figure 4 [29].

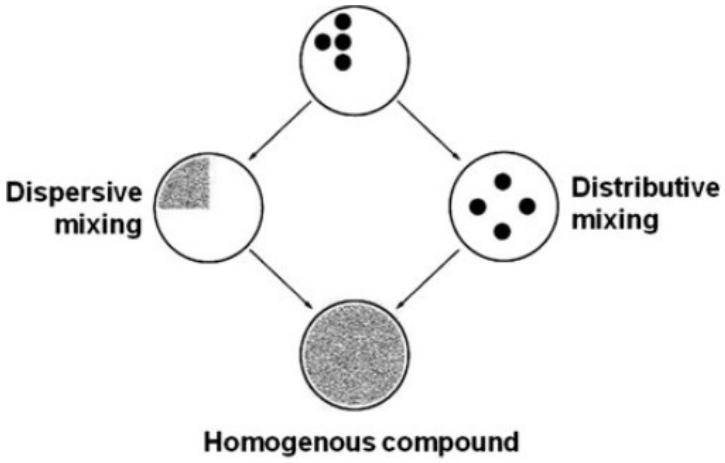

Figure 4. *Dispersive and distributive mixing [29].*

3.2 Single-screw extruders

Most commonly used single-screw extruders can be divided into three geometrical zones: feed section, compression section and metering section. These sections can also be named by the functions they provide. All sections have their own purpose in extrusion process [2,26-28]. The geometrical sections and the most important elements of a typical single-screw extruder are presented in figure 5 [28].

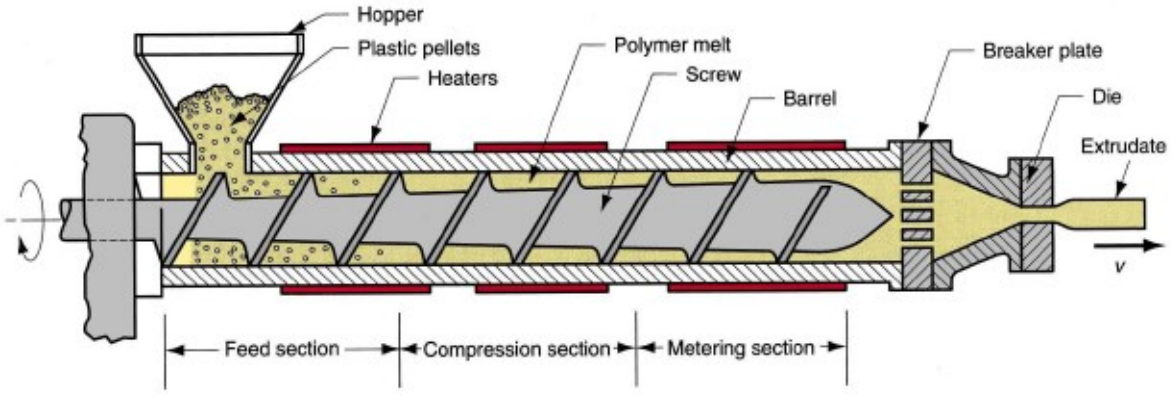

Figure 5. *Schematic of a plasticating single-screw extruder [28].*

The feed section, which can also be called the solids conveying zone, is the first one. The main task of this section is to move the polymer material from the hopper to the screw channel. The friction factor between the polymer and the extruder barrel and the friction factor between the polymer and the extruder screw have a big effect on the material conveying. The process to compact and transport the material will be successful if the friction at the barrel surface is bigger than the friction at the screw surface. This causes the material to move in axial direction, instead of just rotating with the screw. The simplest way to ensure high friction between the polymer and the barrel is to use a grooved feed section. In this design, the barrel surface has grooves in it. In grooved feed section the length of

the grooved barrel is carefully designed to avoid excessive pressures. The feed section is also cooled, usually by cooling lines with cold water flowing in them [2,26-28].

The compression section, which can also be called the melting zone, is the next section of an extruder. Melting of the processed material occurs in the compression section. Melting occurs mainly because of internal friction caused by the rotating screw, which then causes heating. Barrel heaters are also typically used, but their proportion to the total heating is usually much lower than the frictional heating. This is mainly because of low thermal conductivity of polymers [2,26-28]. Melting occurs usually by dissipative melting. In dissipative melting, the size of solid bed of material is getting smaller, as melt pool is forming next to it [26,28]. This effective melting mechanism is illustrated in figure 6a [26].

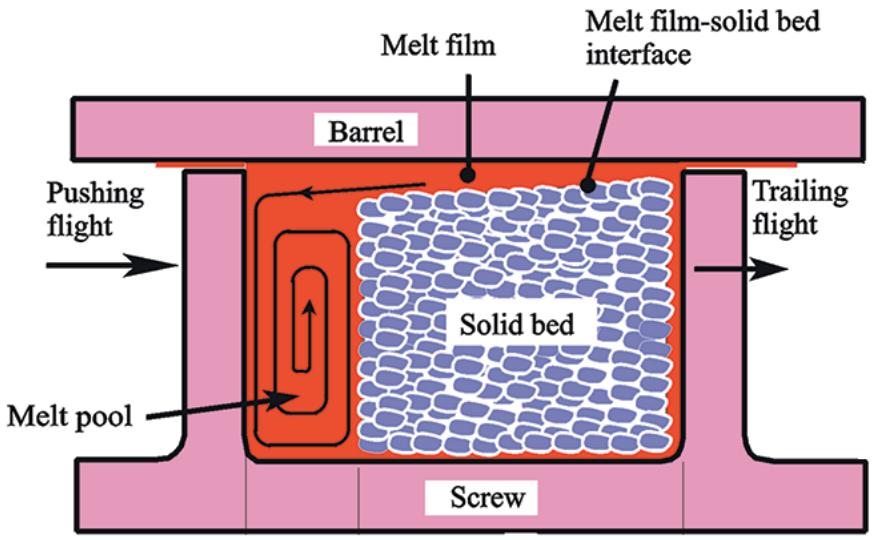

Figure 6a. *Dissipative melting occuring in the extruder [26].*

As melting advances, the solid bed becomes smaller. At some point during melting, the solid bed cannot maintain its structural integrity and uncontrolled solid bed break-up occurs causing the solid bed to break up in smaller pieces [27,28]. The size of these pieces is important, as it takes longer time for bigger particles to melt. At this point another melting mechanism takes place. Conduction melting melts these small unmolten pieces in the melt pool. Conduction melting is not as effective melting mechanism as dissipative melting. That is why the solid bed break-up should be avoided [26,28]. Conduction melting after solid bed break-up is illustrated in figure 6b [26].

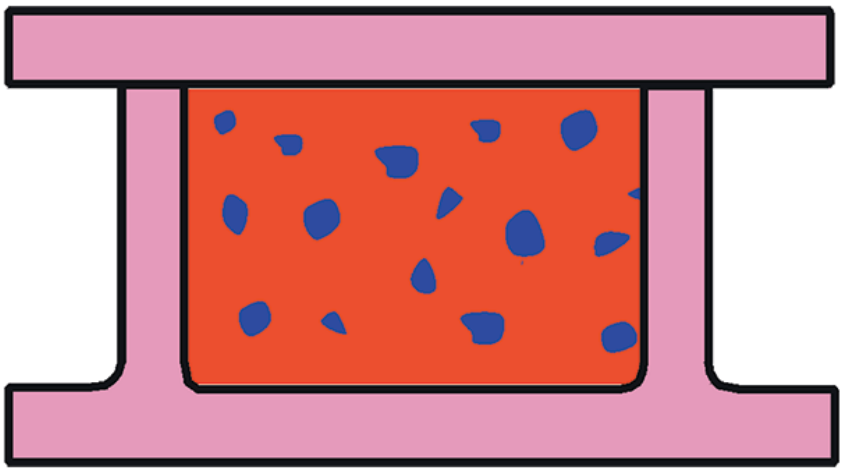

Figure 6b. *Conduction melting occuring in the extruder after solid bed break-up [26].*

Best way to avoid solid bed break-up in single-screw extrusion, is to use a barrier-screw. Barrier-screw separates the solid bed from the melt pool. Barrier typed designs also have good mixing properties [26,28].

The metering section is the last section in the screw. At the end of this section the polymer material should be completely molten and homogeneous. This section can also contain a design of mixing element, to make sure that the melt is homogeneous and in uniform temperature [26,28].

3.3 Twin-screw extruders

Twin-screw extruders provide the best mixing properties from the continuous mixing devices available. Twin-screw extruders can be further classified into counterrotating or corotating twin-screw extruders. Other classification can be done with intermeshing or non-intermeshing twin-screw extruders [2,27].

Twin-screw extruders design requires different linkages and barrels compared to single-screw extruder. In intermeshing twin-screw extruder, the material moves from screw to screw and from flight to flight. The material moves forward with this continuous pumping pattern [2].

There are two possible rotating patterns for intermeshing twin-screw extruders. In corotating pattern, both screws rotate clockwise or both screws rotate counterclockwise. In counterrotating system, screws are rotating in countering directions, meaning that the other screw rotates clockwise and the other rotates counterclockwise. Corotating and counterrotating screws are illustrated in figure 7 [29]. Corotating geometry is the upper screw and counterrotating geometry is the lower screw.

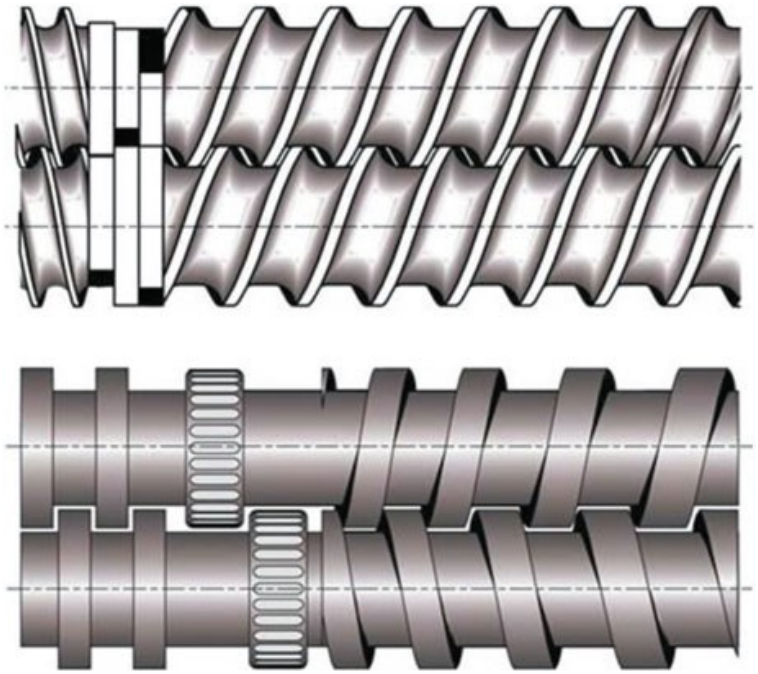

Figure 7. *The geometries of corotating (upper) and counterrotating (lower) twin-crew extruders [29].*

In corotating systems, the material is passed from one screw to another and the material is thus going over and under the screws. Because of this path, most of the material is subjected to same kind of shear as it passes between the screws and the barrel. This also ensures high contact with the extruder barrel and affects the thermal heating. This path is illustrated in figure 8 [30]. Mixing is better in corotating systems than in counterrotating systems. In counterrotating systems, the total shear is lower than with corotating systems, but the counterrotating systems can generate high stresses [2].

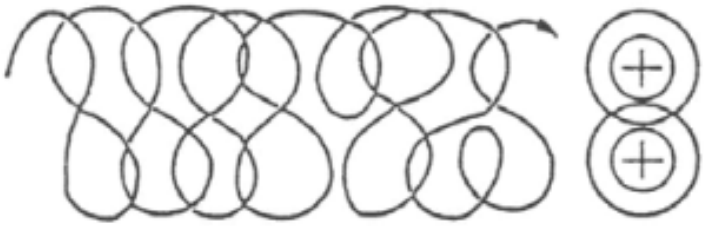

Figure 8. *The material path in intermeshing corotating twin-screw extruder [30].*

4. GRAPHENE

Graphene is one single layer of graphite, in which the carbon atoms are sp^2-bonded in a honeycomb lattice [4,31]. Graphene and other materials that are based on graphene have attracted research attention because of their unique properties, like large surface area and great electrical, thermal and chemical properties. This causes a great potential in different applications [4].

4.1 Preparation of graphene and graphene oxide

Graphene can be obtained by using different techniques, one of the most common being Hummers' method [4]. In this method the graphite is oxidized by using a solution of potassium permanganate in sulfuric acid. This process results to graphite oxide, which can be further exfoliated. Graphite oxide has a similar layered structure to graphite, but there are oxygen-containing groups, like hydroxyl and epoxy, at the plane of carbon atoms. These oxygen groups expand the interlayer distance and make the atomic-thick layers hydrophilic. There are also other oxygenated functional groups, like carbonyl and carboxyl, at the edges of the structure [4,32]. Hummers' method can be continued by using ultrasonication, which causes the oxidized layers to be exfoliated in water. This modification of Hummers' method leads to graphene oxide (GO), a highly oxidized version of graphene [4]. Route from graphite to graphene oxide is presented in figure 9 [33].

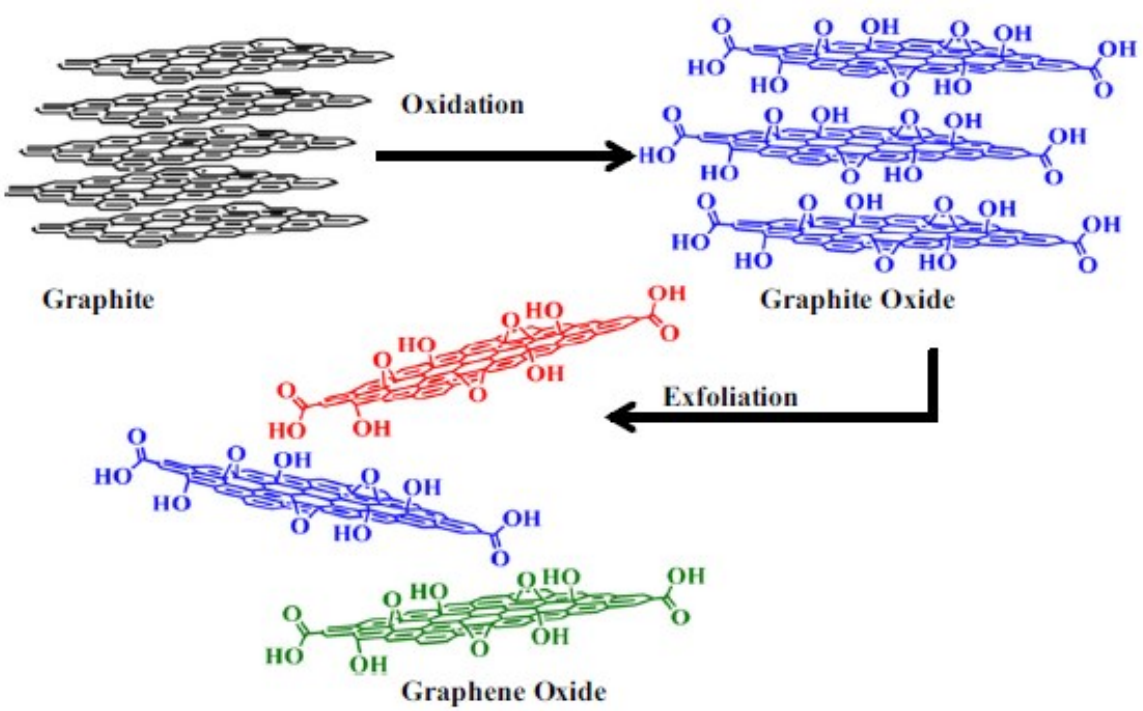

Figure 9. *Route from graphite to graphene oxide [33].*

The modification of Hummers' method is an interesting technique in terms of producing larger quantities of material, but there are also many other methods for producing graphene [32,34]. These methods are usually based on either exfoliation or growth on surfaces. Exfoliation methods include techniques like micromechanical exfoliation and liquid phase exfoliation. Growth on surfaces include methods like epitaxial growth and chemical vapor deposition (CVD). Graphene with a relatively perfect structure and properties can be produced for example by micromechanical exfoliation, epitaxial growth or CVD [34]. In micromechanical exfoliation, graphene is extracted from graphite by using an adhesive tape. Epitaxial growth method is based on thermal treatment of a SiC-crystal under a vacuum. In CVD, graphene is grown on a metal substrate, which is exposed to a gaseous compound [35]. Also, other methods like solution dispersion or mechanical rubbing are possible ways of producing graphene. Some of the possible methods are presented in figure 10 [36].

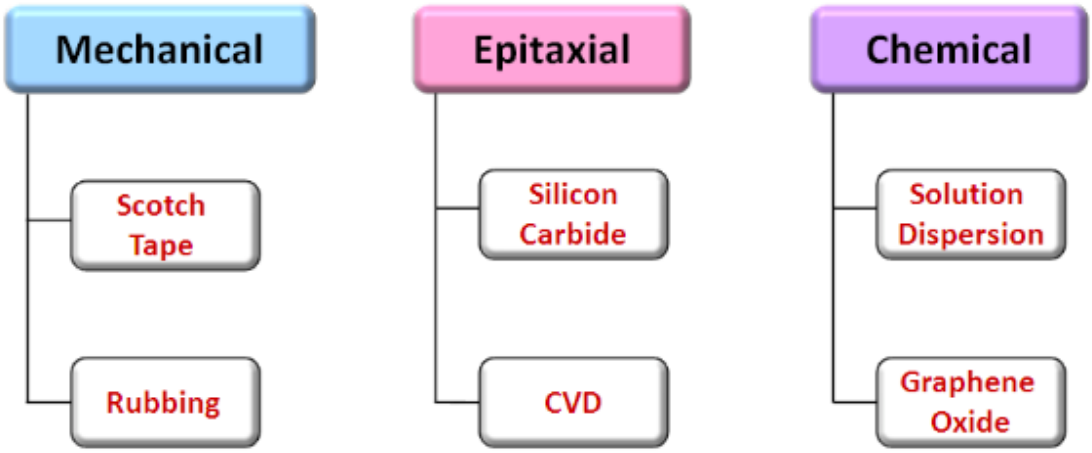

Figure 10. *Methods to obtain graphene [36].*

4.2 Reduced graphene oxide

GO is single-atomic-layered material comprising carbon, hydrogen and oxygen molecules. GO can also be reduced to graphene-like sheets. This happens by the recovery of conjugated structure and by reducing or diminishing the amount of the groups that contain oxygen. This reduction of oxygen-containing groups leads to reduced graphene oxide (rGO), which can also be called functionalized graphene or chemically modified graphene. The reduction causes different properties in rGO compared to GO. Producing of rGO by reducing GO is a very important process because it has great effect on the properties of rGO. This process determines how close the rGO will come to the structure of pristine graphene, which is the main goal of these reduction techniques. These reduction techniques are exploited because producing graphene straight is difficult. This reduced material usually has some properties like pristine graphene, but differences are still substantial, mainly because all the oxygen-containing functional groups can not be removed

from rGO with reduction techniques. The reduction can be done with numerous different methods, but they are all based on chemical, thermal or electrochemical means [4].

4.2.1 Reduction methods

In thermal annealing process, GO is reduced by using high temperatures, which have been achieved by rapid heating [4,32]. Exfoliation of GO also takes places during this reduction process. Exfoliation happens in the process because of CO and CO_2 gases are rapidly evolving in the graphene interlayers. These gases are a result formed from the oxygen containing functional groups of GO. This forming of the gases also causes pressure to increase in the interlayers of GO. As this pressure achieves high levels, it increases the distance of GO sheets and in that way causes exfoliation. This reduction process is usually done under vacuum or protective gas, like hydrogen [32]. Recent research has revealed that removing oxygen groups from GO is possible in lower temperatures also. Reduction in lower temperatures obviously removes fewer groups than high temperature reduction, but sufficient levels can still be achieved [37,38].

Electrochemical reduction is based on electron exchange with GO and electrolyte. There are several different techniques exploiting electrochemical reduction. Typical ways include reducing of aqueous colloidal suspension of GO. This is done in the presence of buffer electrolyte and rGO is formed in the surface of electrode. Another typical way includes thin films of GO, which are used to coat electrode. The coated electrode is then electrochemically reduced in a normal three electrode system [32].

Chemical methods can also be exploited in reduction of GO. The most used method of these chemical reduction methods includes the use of hydrazine [32], but also many other organic and inorganic reducing agents can be exploited [39]. The chemical reduction methods are the most interesting ones for larger scale operations [32,39].

4.3 Functionalization

Functionalization is usually the best way to produce the best performance available from graphene or GO. Functionalization is also sometimes required, if graphene is combined with other materials. Functionalization is achieved by covalent bonds or non-covalent interactions [40]. The covalent functionalization exploits different “grafted from” or “grafted to” techniques [41,42]. However, the covalent functionalization techniques generally compromise the sp^2-structure of graphene. This results to defects in the structure and can affect some properties in a negative way [40-42].

Non-covalent functionalization does not alter the structure of graphenic materials, like covalent functionalization does. Non-covalent functionalization introduces chemical functional groups on the surface of graphene or GO. Electron donor – acceptor complexes, π-π interactions, CH-π interactions, hydrogen bonding and van der Waals forces

are examples of non-covalent functionalization. Non-covalent interactions have positive effect on properties like biocompatibility, reactivity and dispersibility [40].

Non-covalent interactions are present in all materials that experience attractive or repulsive forces [40]. The relative strength of single non-covalent interaction is normally small compared to covalent bonds. Non-covalent interactions combined over large surfaces can, however, have decent dissociation energies, which are comparable to the dissociation energies of some covalent bonds [40,43].

4.4 Properties of graphene oxide and reduced graphene oxide

GO and rGO are an important topic of graphene research because of their properties and characteristics. One of the most important things is that GO can be produced from graphite, which is a cheap and plentiful material. Other important properties of GO include its easy dispersibility in water and organic solvents. GO also has easy dispersibility in polymer matrices. This is an important property when mixing GO with polymer matrices, for example to try to improve the mechanical properties of polymer. Because some of the oxygen groups are removed from rGO, its dispersibility is much worse than GO's. However, because of rGO's structure, it is possible for rGO to interact with different polymer structures. That property creates the possibility to exploit rGO as a compatibilizer. GO is also an electric insulator whereas rGO and graphene have good electrical conductivity. The different kind of functionalization of GO has a large impact on the properties of GO and that is also why there could be potential adaptability for different applications [4]. The applications where GO and rGO are currently being exploited or researched include: electronics devices, energy storage devices, biomedical applications, water purification, coating technology, composites and paper-like materials [4,40].

4.5 Methods of producing graphene-based polymer composites

When creating graphene-based polymer composites, the properties of the final product depends on many things. The homogenous dispersion of graphene into the polymer matrix is one important factor. Also, the interfacial interaction with graphene and polymer matrix have a large role on the final product's properties [44,45].

Three different techniques can be exploited to achieve good dispersion of graphene into polymer matrix. The three methods include solution blending, *in situ* polymerization and melt processing. All of them can be exploited with polyolefins, polyamide and many other polymer matrices [44,45].

4.5.1 Solution blending

Solution blending is the most used method for creating polymer composites. In solution blending process, graphene and matrix polymer are mixed in a solvent. In the process, graphene is usually dispersed in a solvent, then it is mixed together with the polymer solution. The dispersion of graphene in polymer matrix is enhanced with mixing. In the last part of the process, the nanocomposite is recovered either by precipitating by using a non-solvent of the polymer or casting a film [44,45].

Solution-based methods have some advantages compared to others. One of them is, that usually the mixing produces good dispersion of graphene because of low viscosity of the solution. However, a big problem with solution-based methods is that a large amount of solvent must be used [44].

4.5.2 *In situ* polymerization

In *in situ* polymerization, the graphene derivatives are incorporated during the polymerization process. By exploiting this method, it is possible to create composites with covalent linkage between the matrix and the filler. *In situ* polymerization is an important method for insoluble and thermally unstable polymers, which cannot be processed by solution or melt compounding. *In situ* polymerization is also the only method where the dispersion of filler is achieved without a prior exfoliation step in the process. One big advantage of this technique also is, that the formed polymer nanocomposites have the graphene platelets delaminated at nanolevel. This leads to the dispersion being good with the composites created by using *in situ* polymerization [44,45].

4.5.3 Melt processing

In melt processing the polymers are usually processed in pellet form. In this method, the polymers are melted with the help of high processing temperature, which leads to a viscous liquid. High shear forces of the process are utilized to disperse the nanofillers in the polymer matrix [44,45].

Good thing about this method is, that it is cost effective. This is also a good technique for industrial applications, since it is highly compatible with the processed used in industrial scale. It also does not require solvents to be used for the dispersion process thus making the process simple, compared to other methods [44,45].

5. MATERIALS AND METHODS

This section has information about the materials that were used during this thesis. Also, information about the laboratory work, the processing equipment and parameters is listed. Furthermore, information about the used analyzing equipment and programs is provided.

5.1 Materials

LDPE purchased from Borealis Polymers Oy, Finland was used as a matrix. Zytel® 101F NC010, internally lubricated PA66 resin purchased from DuPont, Finland was used as a minor component. Sulfuric acid (H_2SO_4) purchased from VWR International Oy, Finland, sodium nitrate ($NaNO_3$) purchased from Sigma Aldrich, Germany, graphite powder purchased from TIMCAL Ltd., Switzerland, potassium permanganate ($KMnO_4$) purchased from Merk, Germany and hydrogen peroxide (H_2O_2) purchased from Sigma Aldrich, Germany were used in Hummers' method. Formic Acid 98 – 100 %, for analysis, (HCO_2H) purchased from Sigma Aldrich, Germany was used in etching. Toluene (C_7H_8), Acetone (C_3H_6O) and distilled water were also used during the experimental part of this thesis.

The different materials and the working phases in which they were used in have been sorted out in table 2.

Table 2. *Different materials that were used in different phases of the work.*

Work phase	Material
Modified Hummers' method (producing graphene oxide)	Sulfuric acid, H_2SO_4 Sodium nitrate, $NaNO_3$ Graphite powder Potassium permanganate, $KMnO_4$ Hydrogen peroxide, H_2O_2 Distilled water
Preparing a masterbatch	LDPE Graphene oxide Acetone, C_3H_6O Toluene, C_7H_8
Processing	LDPE PA66 Graphene oxide
Etching	Formic acid, HCO_2H

5.2 Modified Hummers' method

Modified Hummers' method was used to manufacture GO. This method provides a way for synthesis of GO from graphite.

1. Ice bath was prepared.
2. 46 ml of sulfuric acid was measured in a 500 ml volumetric flask. Volumetric flask was placed into ice bath at 0 ºC to cool the sulfuric acid while constantly being stirred by a bar magnet.
3. 0,1 g of sodium nitrate was mixed with sulfuric acid with constant stirring.
4. 2 g of Graphite powder was slowly mixed into the reaction with constant stirring.
5. 6 g of Potassium permanganate was very slowly added into the reaction mixture. The temperature was maintained at 0 – 5 ºC during the addition of potassium permanganate.
6. Ice bath was removed, and the mixture was continuously stirred at 25 ºC for a minimum of 6 hours. This results a thick paste.
7. 92 ml of distilled water was added followed by continuous stirring. The temperature of the mixture increases to approximately 90ºC with the addition of water.
8. Mixture was stirred for 0,5 hours and 280 ml of distilled water was added to it.
9. 3 ml of 30 % hydrogen peroxide was added to the mixture after a while. This causes color change from dark brown to yellow.
10. The obtained product was filtrated through filter paper with the help of a pump to provide suction.
11. The fraction was collected from the filter paper and re-dispersed in distilled water.
12. The obtained product was then centrifuged. Bottom fraction was collected from the centrifuge and re-dispersed in distilled water. The procedure was repeated several times until the pH of the supernatant solution was approximately 7. The pH was determined by pH paper. Sonication was always used in between centrifugations.
13. GO was obtained by collecting the bottom fraction from the centrifuge.

The mixture was poured into several Petri dishes for drying. The material was dried in an oven for 12 hours at 50 ºC. The dried product was detached from the surface of the Petri dishes with the help of a surgical knife. The GO film detached from the Petri dish is presented in figure 11. The figure also presents smaller parts of the film, which have been cut and placed into a glass sample vial.

Figure 11. *GO film and smaller parts of the film.*

The detached GO was then collected, and the film was cut and grinded into a fine powder by using a mortar and pestle. This was repeated several times, until enough GO powder was obtained for the processing.

5.3 Preparing masterbatches

The masterbatches were done by using LDPE, toluene, GO and acetone. Two batches were prepared. First with 1 wt% of GO and the second with 2 wt% of GO. The GO amount in the two masterbatches were naturally different, but otherwise the procedure remained the same.

1 g of LDPE granules and 28 g of toluene was weighted and then placed into same boiling tube together. Heat was then applied to dissolve the LDPE granules. At approximately 85 ^{o}C LDPE started to dissolve into toluene.

0.04 g of GO was weighted to make the first masterbatch of GO1wt%. In the masterbatch of GO2wt%, the weighted GO amount was 0.08 g. The weighted GO was placed into a mortar and acetone was added. Pestle was used to mix the GO into acetone. The mixture was then placed into a boiling tube and weighted to make sure that acetone amount was approximately 7 g.

The mixture with LDPE granules dissolved in toluene, and the mixture with GO mixed in acetone were then poured into same boiling tube to mix them together. These masterbatches were then carefully poured into several Petri dishes and the Petri dishes were placed into oven to dry. The oven was set to 80 ^{o}C and the masterbatches were left into the oven to dry for several hours. The Petri dishes were then removed from the oven after the masterbatches had dried. The dried material was then removed from the Petri dishes and collected for processing purposes. The bigger film parts were also cut to smaller pieces before processing.

5.4 Processing the samples

Processing was made by using a laboratory scale DSM Xplore 5 twin-screw micro-compounder model 2005. The micro-compounder has a base capacity of 5 cm^3, two conical co-rotating screws with a length of 90 mm, maximum processing temperature of 400 ºC and 6 different heating zones, which can be controlled by operating a touchscreen. The machine also has a recirculating channel in its design. One of the biggest positive sides of this extruder machine is that only a small amount of material is needed for the processing. The machine at Tampere University of Technology (TUT) has been illustrated in figure 12.

Figure 12. *The micro-compounder at TUT.*

The polymer materials that were used in processing were in a granule-form. The PA66 resins were dried in oven for several hours at 80 ºC before processing, to ensure that moisture content was sufficiently low. The first mixing was done by setting the extruder temperature to 265 ºC. All the samples were processed for 5 minutes. First sample was processed without GO. This was done by feeding 0.4 g of PA66 and 3.6 g of LDPE into the extruder. Then two samples with GO were processed. In this processing, the GO was fed into the extruder in a powder form. The amount of GO, in both processed samples, was 0.02 g. The amount of PA66 and LDPE were the same as with pure blend. The extruded materials were then observed visually. The visual inspection confirmed that not much of a color change or other indications of GO's affect were detected in the extruded materials. This was not a surprise, since feeding the GO into the extruder in a powder form was difficult. This was mainly because of the small amount of GO, and because the extruders hopper is designed in a way that it is easier to feed granules and other material with bigger size than fine powder. That caused the fine formed GO powder to not go into the extruder at all. That is why it was decided to use only masterbatches in the future processing runs.

The total amount of polymer materials remained the same when processing the masterbatches. However, as mentioned before, 1 g of LDPE was in the masterbatch with GO1wt%. So, in total 0.4 g of PA66 and 2.6 g of LDPE were in pellet form, but the total amount of polymers remained the same, 0.4 g of PA66 and 3.6 g of LDPE.

The processing time was changed for this processing. This time, the PA66 was first fed into the extruder for 3 minutes before adding the other components. This was done because PA66 has higher melting temperature and processing temperature than LDPE. Total processing time was 8 minutes. Also, the temperature was set up to 270 ºC. A pure blend was processed first without GO. Then PA66, LDPE and masterbatch with 1 wt% of GO was processed. The samples were visually inspected, and the masterbatch result looked more promising than in the first mixing with the powder. The masterbatch was also much easier to feed into the hopper because the size of the film parts was bigger than with the GO powder.

The processing time and temperature were yet again changed for the third processing to ensure good melt mixing. Temperature was set to 280 ºC and processing time was added up to 10 minutes total for the blends. 5 minutes processing time was used for the pure LDPE and pure PA66. In the other samples, the processing time was divided in a way that 5 minutes was used to mix the PA66 and 5 minutes was processed after LDPE and masterbatch were added. Visual inspection showed promising results for the samples with GO content in them, so analyzing methods were then used to analyze the samples further.

The processing was also repeated in the fourth processing with the same exact parameters and material amounts as in the third processing. This was done to ensure that there was enough material for the analyzing methods. This was also done to confirm that the mixing

showed good results and that the parameters used in the processing were good. The material processed in the third processing was however large enough amount for the analyzing methods, so the samples from the fourth processing round remained as a backup material in this work.

As mentioned, the temperature was changed in the processing runs with different samples, but all the samples were processed with a screw-speed of 80 rpm. The total amount of samples that were processed was 15 and this was done with 4 different processing runs. All the processed samples, processing times and processing temperatures are presented in table 3. Table 3 also contains information about the recipe of the materials which were processed. The vertical lines in the table are referring to the ending of a processing trial.

Table 3. *Processed samples with information about the recipe, GO content and the processing.*

Temperature	Mixing time	Sample	Recipe
265 °C	5 min total	Blend	0.4 g PA66 + 3.6 g LDPE
265 °C	5 min total	GO in powder form	0.4 g PA66 + 3.6 g LDPE + 0.02 g GO
265 °C	5 min total	GO in powder form	0.4 g PA66 + 3.6 g LDPE + 0.02 g GO
270 °C	8 min total (3 min after PA66)	Blend	0.4 g PA66 + 3.6 g LDPE
270 °C	8 min total (3 min after PA66)	Blend+GO1wt%	0.4 g PA66 + 2.6 g LDPE +Masterbatch [1 g LDPE + 0.04 g GO]
280 °C	5 min total	Pure PA66	4 g PA66
280 °C	5 min total	Pure LDPE	4 g LDPE
280 °C	10 min total (5 min after PA66)	Blend	0.4 g PA66 + 3.6 g LDPE
280 °C	10 min total (5 min after PA66)	Blend+GO1wt%	0.4 g PA66 + 2.6 g LDPE +Masterbatch [1 g LDPE + 0.04 g GO]
280 °C	10 min total (5 min after PA66)	Blend+GO2wt%	0.4 g PA66 + 2.6 g LDPE +Masterbatch [1 g LDPE + 0.08 g GO]
280 °C	5 min total	Pure PA66	4 g PA66
280 °C	5 min total	Pure LDPE	4 g LDPE
280 °C	10 min total (5 min after PA66)	Blend	0.4 g PA66 + 3.6 g LDPE
280 °C	10 min total (5 min after PA66)	Blend+GO1wt%	0.4 g PA66 + 2.6 g LDPE +Masterbatch [1 g LDPE + 0.04 g GO]
280 °C	10 min total (5 min after PA66)	Blend+GO2wt%	0.4 g PA66 + 2.6 g LDPE +Masterbatch [1 g LDPE + 0.08g GO]

As presented in table 3, in this work the samples with only LDPE and PA66 are referred as blend. The samples made with the first masterbatch, containing LDPE, PA66 and 0.04 g of GO are referred as blend+GO1wt%. Finally, the sample made with the second masterbatch, containing LDPE, PA66 and 0.08 g of GO is referred as blend+GO2wt%.

5.4.1 Pressing the samples

After the processing, the samples were pressed into a film form. The press that was used was a hydraulic press with two square plateaus. The side length of the plateaus in this machine is 15 cm. In this work phase, the samples were first cut to smaller pieces to make the pressing easier. The cut sample pieces were then placed in the lower plateau of the press. The press that was used has several thermal elements in its plateaus. The elements in the upper and the lower plateau were set on the same temperature as the samples were processed in, 280 ^{o}C. This ensured the melting of the samples. The pressure that was used to press the plateaus together was 6 bars. The setup of the hydraulic press and the controls for the thermal elements are presented in figure 13.

Figure 13. *The press setup at TUT.*

5.5 Etching

Etching was done to the samples to get information about the dispersion of PA66 in the LDPE matrix in different blends. This was an important work phase, so the samples could be further analyzed and compared with the use of Field Emission Scanning Electron Microscope. The acid that was used in the etching process was formic acid (HCO_2H) 98 – 100-% from Sigma Aldrich.

One sample of blend, one sample of blend+GO1wt% and one sample of blend+GO2wt% were prepared for the etching. The samples were cut from the larger films, which were prepared with the press. The samples were selected in a way that the material that was cut was a representative sample of the larger film. These samples were then placed in three different glass vials. The formic acid was then added to the vials in a way that the samples

were covered in acid. The samples were left in the acid for 72 hours. After that, the samples were carefully removed from the acid for further analyzing.

5.6 Characterizations

Different characterization methods were used to gain qualitative and quantitative information about the different blends. The blends were usually compared with each other, but also the information that was gained from pure LDPE and pure PA66 samples was exploited when different analyzing methods were used.

During this work a broad scale of different methods were utilized to gain as much information as possible. These methods include, X-Ray Diffraction (XRD), Field Emission Scanning Electron Microscope (FESEM), Differential Scanning Calorimeter (DSC), Thermogravimetric Analysis (TGA) and Fourier Transform Infrared spectroscopy (FTIR).

5.6.1 X-Ray Diffraction (XRD)

In XRD X-rays interact with crystalline phase of a substance. This provides a diffraction pattern, which can be identified. In this work XRD was used to evaluate the interlayer changes and crystalline properties of the measured samples from their diffraction patterns. XRD measurements were carried out by using Panalytical Empyrean Multipurpose Diffractometer with CuK_α radiation ($\lambda = 1.542$ Å). It was operated at 45 kV and 40 mA. XRD measurements were recorded in 2θ values of 5^o - 50^o and with a scan rate of 5 ^{o}/min. XRD was used to evaluate the GO powder and the film samples. When evaluating the GO powder, the powder was evenly spread in the round sample holder. Same sample holder was used to evaluate the film samples. When the film samples were evaluated, they were cut in representative size and uniform thickness and were then placed into the sample holder.

5.6.2 Field Emission Scanning Electron Microscope (FESEM)

FESEM is an analytical technique where electrons are released from a field emission source. FESEM provides large magnifications from the surface of substances. The FESEM images were inspected to gather information about the dispersion of PA66 into the LDPE matrix. This was done to different samples also to evaluate graphene oxides affect to the dispersion. The samples were examined by using a Scanning Electron Microscope Zeiss ULTRAplus. The studied etched films were glued with a carbon glue to a sample holder and coated with a thin carbon layer to ensure the conductivity.

5.6.3 Differential Scanning Calorimeter (DSC)

DSC is a thermal analyzing method based on the difference in heat flow to sample and to reference. The heat flow is monitored against time and temperature as suitable temperature program is applied to analyze the sample. The DSC measurements in this work were performed to gain information about enthalpy changes, crystallization and compatibility between components. DSC measurements were conducted by using Netzsch DSC 214 Polyma under flowing nitrogen. The samples with approximately same mass were researched with the same temperature program. In the program, the samples were first heated from -30 ºC to 300 ºC with a heating rate of 10 ºC/min. Then the samples were cooled down to -30 ºC with a cooling rate of 10 ºC/min and held there for 10 minutes. In the final step the samples were reheated to 300 ºC with a heating rate of 10 ºC/min. The first heating was done to remove the thermal history of the sample, the second heating shows the real thermal response of the studied sample. The temperature program is illustrated in figure 14.

Nr	Type	°C	K/min	Time	pts/min	pts/K	AC	O2	N2	N2
1		30.0	10.000				1	0	40	60
2		30.0		0:15:00			1	0	40	60
3		30.0		0:01:00	300.00		1	0	40	60
4		-30.0	10.000	0:06:00	300.00	30.00	1	0	40	60
5		-30.0		0:10:00	20.00		1	0	40	60
6		300.0	10.000	0:33:00	300.00	30.00	0	0	40	60
7		-30.0	10.000	0:33:00	300.00	30.00	1	0	40	60
8		-30.0		0:10:00	300.00		1	0	40	60
9		300.0	10.000	0:33:00	300.00	30.00	0	0	40	60
10		310.0					0	0	40	60
11		30.0	50.000	0:05:24			1	0	40	60
12		30.0		2:00:00			1	0	40	60

Figure 14. *The temperature program that was used in DSC analysis.*

5.6.4 Thermogravimetric Analysis (TGA)

TGA is a thermal analyzing method. In this method the change of sample mass is monitored as a function of temperature. That is why factors like heating rate, sample mass and thermal conductivity of the sample affect the results gained from TGA. In this work TGA was used to characterize the thermal stability of the samples. TGA measurements were performed by Netzsch TG209 F3 Tarsus. Samples with approximately same mass were heated from 30 ºC to 700 ºC at a heating rate of 10 ºC/min, under flowing nitrogen.

5.6.5 Fourier Transform Infrared spectroscopy (FTIR)

FTIR is an analytical method, which can be exploited in identifying different materials. In this method the samples absorption of infrared radiation versus wavelength is measured. The wavelengths absorbed by the sample are characteristic to the samples molecular structure. The interactions with GO and LDPE and the interactions with GO and PA66 were studied with FTIR analysis. FTIR measurements were done by using Bruker Optics Tenson 27. The measurements were done with attenuated total reflectance and with the spectra were recorded between 4000 cm^{-1} and 500 cm^{-1}.

6. RESULTS AND DISCUSSION

In this section, all the results, graphs and data from different analyzing methods are presented. Also, some of the graph results are presented in tables. This is done because some calculations are in order, to present the useful information in different charts in a clearer way. The results are mostly presented in the order that the analyzing methods were used during the experimental part of the work. Although some methods, like XRD measurements, were performed in different parts of the work.

The results from different analyzing methods are presented and discussed in this section of the work. The results are considered mostly in comparison between blend, blend+GO1wt% and blend+GO2wt%. Also, some comparison between pure LDPE and pure PA66 is made. This seemed to be the best way to assess the results, and changes that happened with the addition of GO to the blends.

Many methods were exploited to get results from broad scale. Main focus of the results is on thermal properties, dispersion of the components in the matrix and chemical interactions in the samples.

6.1 XRD results

XRD was first used for the analysis of the GO powder. This was done to confirm, that the modified Hummers' method had been successful, and the produced GO was what it was expected to be. The characteristic diffraction peak of graphite at around $2\theta = 26°$ is replaced by a sharp peak at the position of approximately 11° in the pattern for GO. This indicates that the oxygen functional groups, like carbonyl and hydroxyl groups, are inserted into the graphite layer. This confirms the successful oxidation of GO [46]. The peak at approximately 11^{o} can also be seen in figure 15a.

XRD patterns of GO, blend, blend+GO1wt%, blend+GO2wt% and pure PA66 are presented in figure 15a and figure 15b. Figure 15a is limited in between 5^{o} and 40^{o}. This means that the GO peak is visible in this area. It can also be seen that the characteristic sharp peak of GO is not visible in the samples of blend+GO1wt% and blend+GO2wt%. This is expected, if GO is uniformly dispersed into the matrix of the samples. The dispersion would then cause the peak to disappear because the crystallographic order is lost. The dispersion is also seen in the SEM results presented in figure 16. Similar disappearance of the peak has been witnessed by other studies with graphenic materials as well [47].

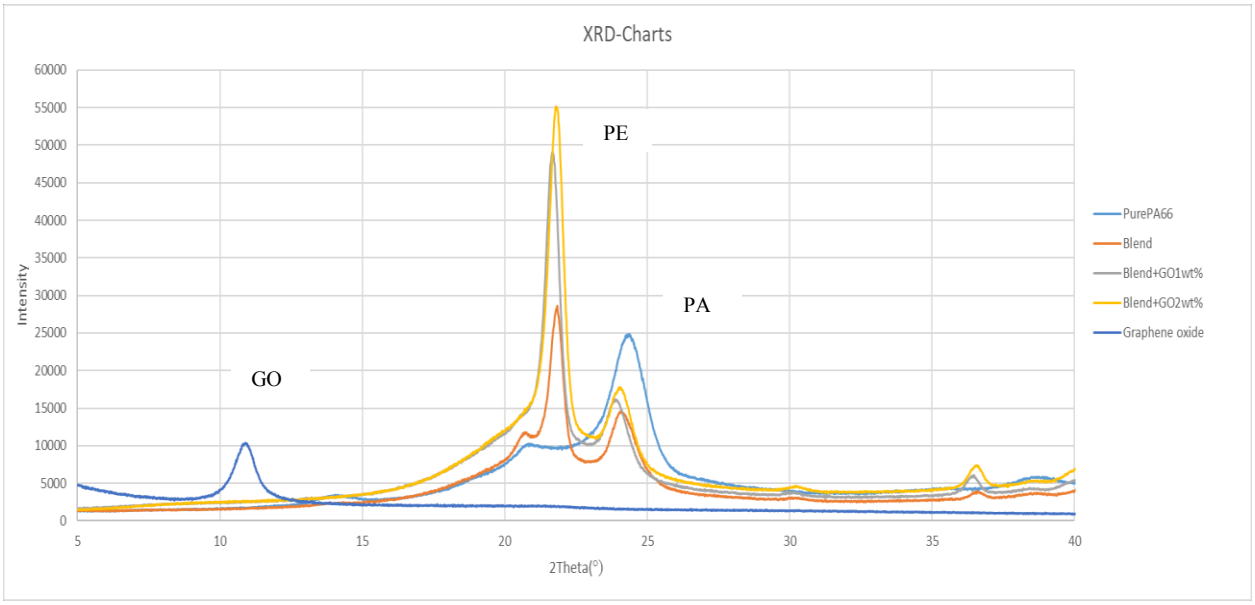

Figure 15a. *XRD patterns for GO powder, blend, blend+GO1wt%, blend+GO2wt% and pure PA66 in the 2Theta(º) area of 5º - 40º.*

In XRD results it can also be seen that two big peaks occur with the samples. These are presented in figure 15a, PE referring to the peaks at approximately 21º and PA referring to the peak at approximately 24º. The GO peak is also marked in the figure. There is also a smaller peak visible in the pure PA66 pattern and in the blend pattern. The peak is visible at around 21º area and it looks more like a shoulder than a sharp peak. This peak is not seen in the blend+GO1wt% pattern and in the blend+GO2wt% pattern. This peak is visible in both figure 15a and figure 15b, but it can be seen more clearly in figure 15b because figure 15b is limited in between 16º and 26º to highlight the shifting happening in the peaks of the samples. The peak is most likely caused by PA66, which then disperses better into the LDPE matrix with GO as a compatibilizer causing the change in crystalline phases. This would then cause the peak to disappear from both samples that have GO in them.

The major two peak positions are changing with different samples. This peak shifting is caused by different laminar spacing in crystalline phases of the sample. There is also a change in the peak intensity of the different materials. In the PE peaks area, the intensity of the peaks gets higher as the GO content is larger. In the PA peaks area, the intensity is also increasing as the GO content is getting bigger. As the diffraction peaks are getting higher values with the increasing GO amount, it indicates that the crystallization is increasing with the addition of GO to the blend. This peak shifting can be seen in figure 15a and in figure 15b.

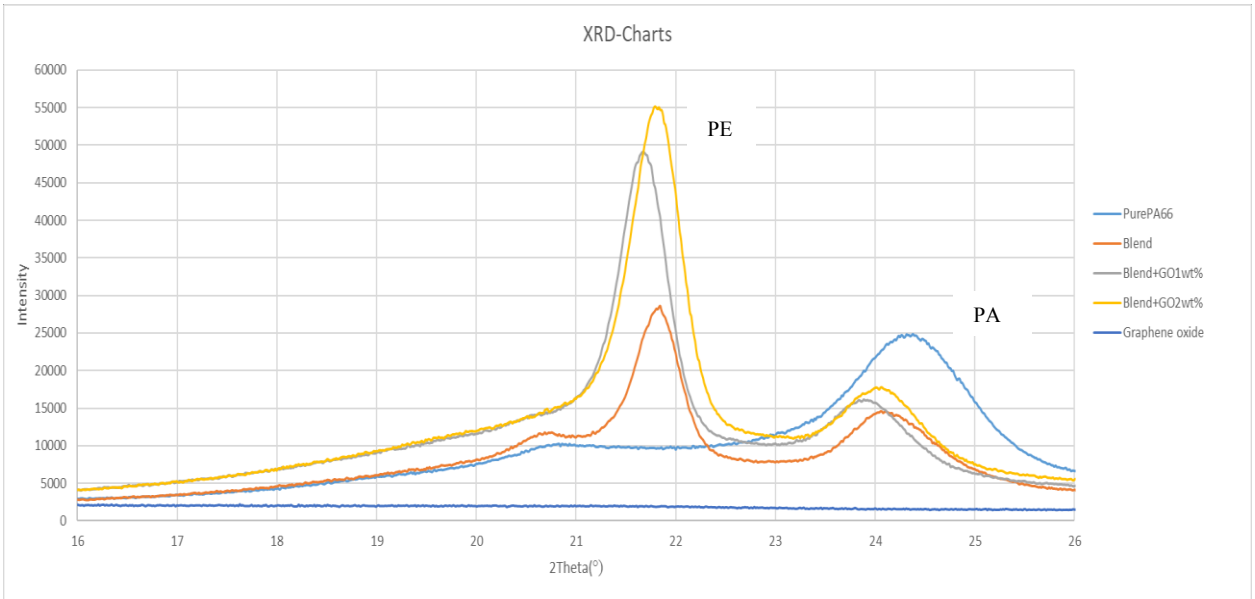

Figure 15b. *XRD patterns for GO powder, blend, blend+GO1wt%, blend+GO2wt% and pure PA66 in the 2Theta(°) area of 16° - 26°.*

In figure 15b the different peaks in the blend, blend+GO1wt%, blend+GO2wt% and the single peak in PA66 can be seen clearly. The peak shifting which happens with different blends and with PA66 can be determined further by using Bragg's law. These calculations are performed out of interest in the numerical values, no additional information is necessarily gained since the shifts are already visible in the XRD charts.

6.1.1 Results from Bragg's law

Bragg's law can be applied when analyzing the XRD data further. In this way, more precise numerical information can be shown as an addition to the XRD patterns.

$$\lambda = 2\mathrm{d} * \sin(\theta) => d = \frac{\lambda}{2\sin(\theta)} \tag{3}$$

where, λ is the wavelength of the X-ray beam, θ is the diffraction angle, which can be received from the XRD data. And finally, d is the distance between adjacent GO sheets.

Bragg's law can be used to calculate the spacing between graphene oxide sheets by using data values are from the XRD data of GO powder.

$$d = \frac{\lambda}{2\sin(\theta)} = \frac{0.154\,nm}{2\sin(5.445°)} = 0.812nm$$

Bragg's law can also be exploited in calculating the data from the peaks of the blend, blend+GO1wt%, blend+GO2wt% and the single peak in PA66. In these calculations, the *d* in the equation represents the spacing of crystalline plane. By using the values from XRD data, calculations can be made.

PE Peak:

$$Blend: d = \frac{\lambda}{2\sin(\theta)} = \frac{0.154\ nm}{2\sin(10.920°)} = 0.406\ nm$$

$$Blend + GO1wt\%: d = \frac{\lambda}{2\sin(\theta)} = \frac{0.154\ nm}{2\sin(10.840°)} = 0.409\ nm$$

$$Blend + GO2wt\%: d = \frac{\lambda}{2\sin(\theta)} = \frac{0.154\ nm}{2\sin(10.895°)} = 0.407nm$$

PA Peak:

$$Blend: d = \frac{\lambda}{2\sin(\theta)} = \frac{0.154\ nm}{2\sin(12.025°)} = 0.370\ nm$$

$$Blend + GO1wt\%: d = \frac{\lambda}{2\sin(\theta)} = \frac{0.154\ nm}{2\sin(11.945°)} = 0.372\ nm$$

$$Blend + GO2wt\%: d = \frac{\lambda}{2\sin(\theta)} = \frac{0.154\ nm}{2\sin(12.035°)} = 0.369\ nm$$

$$PurePA66: d = \frac{\lambda}{2\sin(\theta)} = \frac{0.154\ nm}{2\sin(12.190°)} = 0.365\ nm$$

The results show that the slight shift of the peak position affects the interlayer spacing's in the samples. The peak shifting is already visible in the XRD graphs. These slight shifts are happening in PE peaks area and in PA peaks area. As it can be seen, PA66 only has a peak in the PA66 peak area and naturally the blend, blend+GO1wt% and blend+GO2wt% have peaks in both areas. The results are presented in table 4.

Table 4. *Shifting in the peaks of the blend, blend+GO1wt%, blend+GO2wt% and the PA66.*

Name	Peak	Spacing, d
Blend	PE	0.406 nm
Blend+GO1wt%		0.409 nm
Blend+GO2wt%		0.407 nm
Blend	PA	0.370 nm
Blend+GO1wt%		0.372 nm
Blend+GO2wt%		0.369 nm
PA66		0.365 nm

The result show that the interlayer spacing is changing, when comparing the different blends in area of PE peak. The changes also happen in area of PA peak, when comparing the results from the blend, blend+GO1wt%, blend+GO2wt% and the result from PA66. The shifting of peaks seems to be a good thing, because it shows that GO is affecting the blend.

When comparing the result between blend and blend+GO1wt%, the spacing is increasing in both peak areas as the GO content is added. However, in the results from blend+GO2wt%, the spacing is decreasing in both peak areas. Therefore, it is difficult to draw any precise conclusions about these interlayer spacing results.

6.2 FESEM images

After the etching process, the samples of blend, blend+GO1wt% and blend+GO2wt% were researched with FESEM. In the etching process, the formic acid dissolves the PA66, forming holes into the film, but does not affect the LDPE. This provides a good way to assess the dispersion of PA66 into the LDPE matrix. The PA66 should have better dispersion into the LDPE matrix with the addition of GO, than it would have in a normal immiscible blend. The images are presented in figure 16.

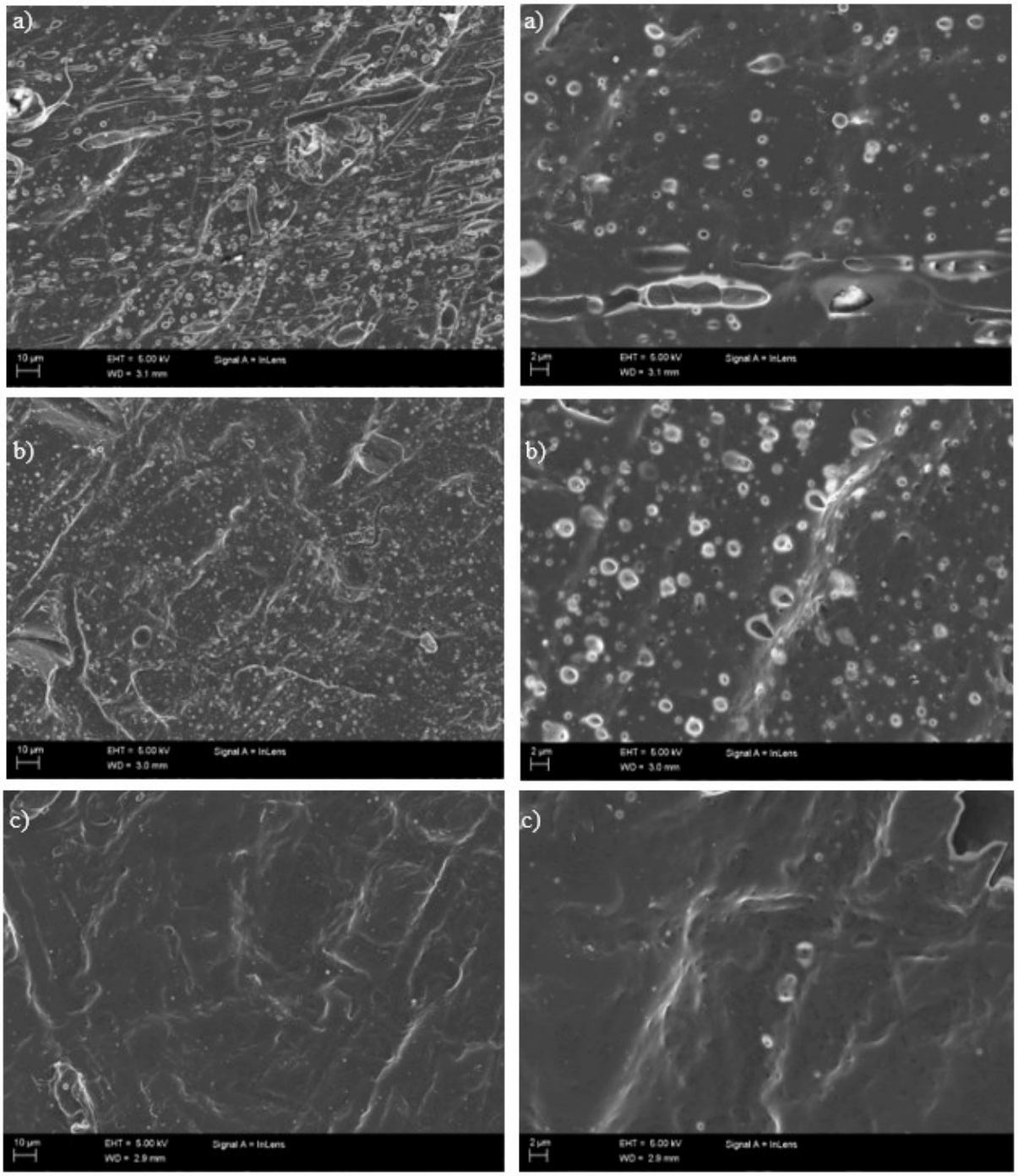

Figure 16. *FESEM images. a) blend b) blend+GO1wt% c) blend+GO2wt%.*

It can be seen from the FESEM images in figure 16, that in the blend, the holes formed by the formic acid are large and can be seen clearly. This is an indication of poor dispersion, which is very typical for immiscible blends. In both a) images there are big holes in the film and the average size of the holes is large and the variation in hole size is big.

In the film formed from blend+GO1wt%, the average size of the holes is smaller compared to the film without GO. No bigger holes can be seen clearly, and the dispersion seems to be dramatically better than with the blend without GO. This can be seen from both b) images.

Finally, in the film formed from blend+GO2wt%, the average size of the holes is still smaller than in the film without GO and in the film with GO1wt%. No bigger holes are visible in the c) images. This would indicate a much better dispersion of PA66 in the LDPE matrix by using GO as a compatibilizer and is a very promising result.

6.3 DSC results

The data collected by DSC is presented in figure 17. The results have been collected from the second heating in the temperature program of the DSC. LDPE and PA66 peaks are marked in the figure to make it more easily readable.

Figure 17 shows that the area of the PA66 peak is getting smaller with the addition of GO into the blends, whereas the area of the LDPE peak is getting larger with the addition of GO into the blends. The complex peak value of the blend+GO1wt% is lower than the value of blend+GO2wt% in the LDPE peak area, so the addition of GO content seems to lower the rate of transformation. Also, the blend without GO has the lowest complex peak value. Because these values of the LDPE peak are increasing with the addition of GO, it could indicate that GO is working as a compatibilizer, since better dispersion would cause the higher value measured in the matrix polymer peak.

It can be seen from figure 17 that there is also some effect on the melting peak of PA66. Without GO it is approximately 261 ^{o}C. Adding GO lowers the peak, with blend+GO1wt% it is approximately 259 ^{o}C and with blend+GO2wt% it is approximately 257 ^{o}C. On the other hand, the melting peaks stay approximately the same in the LDPE peak. All of the peaks are approximately 110 ^{o}C.

There is also a small peak visible in the shoulder of the PA66 peak in the blends result. This small peak is most likely caused by melt re-crystallization of polyamide in the second heating. This can be caused by the slow heating rate that was used in the DSC program [48]. This peak is not there with the blend+GO1wt% and with the blend+GO2wt% so it is only visible in the pure blends graph.

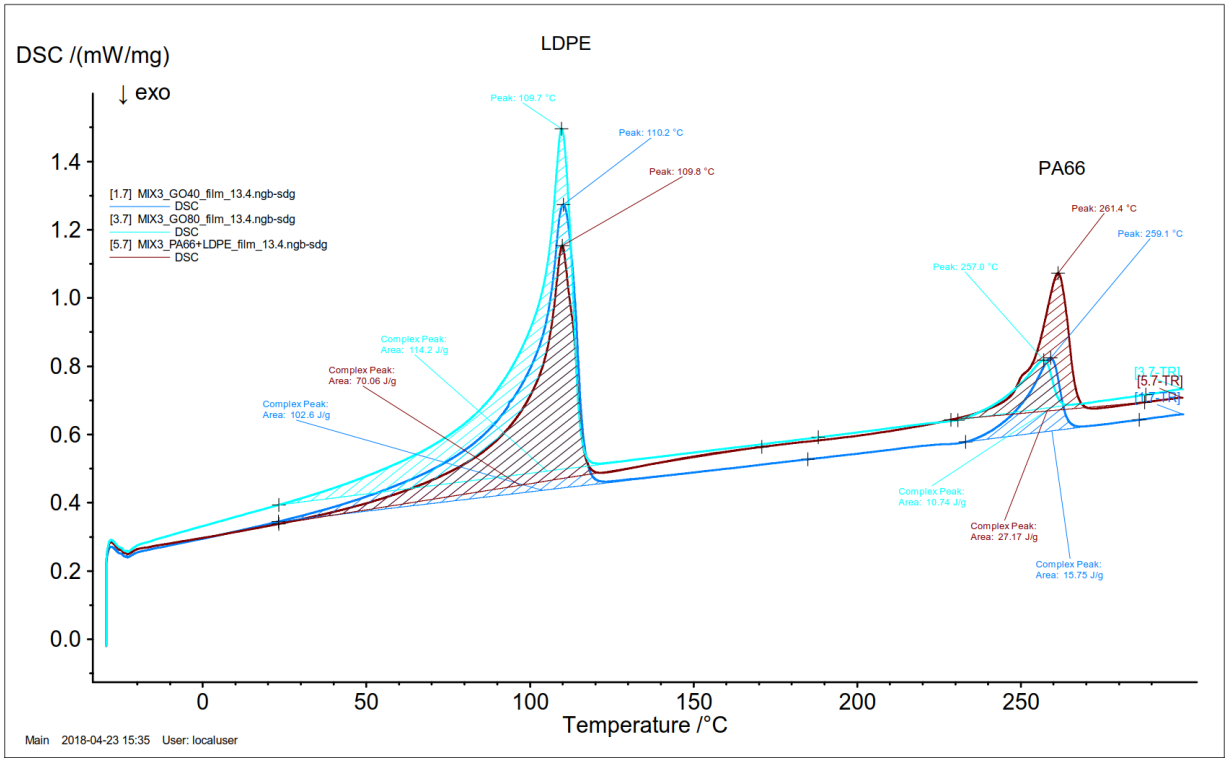

Figure 17. *DSC curves for blend, blend+GO1wt% and blend+GO2wt%.*

The changes can be seen more clearly when analyzing the numerical changes in complex peak areas. The complex peak area values in the LDPE region are 70.0 J/g for the blend, 102.6 J/g for blend+GO1wt% and 114.2 J/g for blend+GO2wt%. In the PA66 region the values are 27.1 J/g for the blend, 15.8 J/g for blend+GO1wt% and 10.7 J/g for blend+GO2wt%. These values are taken straight from the DSC curves made by the DSC program.

The complex peak values of the LDPE peaks are compared in figure 18. The values are presented in the figure as a function of the GO content of the different samples. The figure shows that the growth in the complex peaks with increasing GO content is not linear. The complex peak grows with steeper slope when comparing blend to blend+GO1wt% than when comparing blend+GO1wt% with blend+GO2wt%. This indicates that the first addition of GO has a larger effect on the complex peak than the additional one.

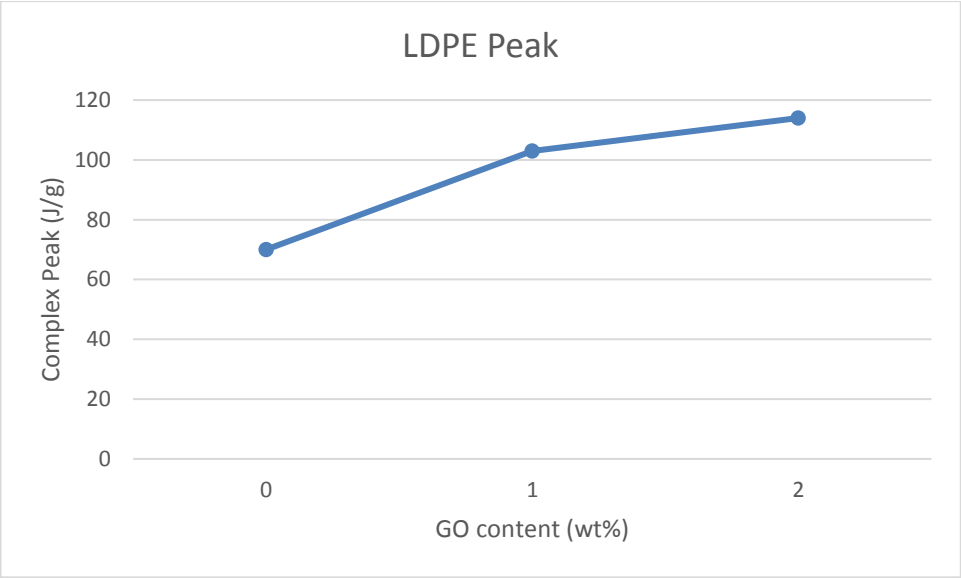

Figure 18. *Complex peak areas as a function of GO content in LDPE peak area.*

The complex peak area values show the same behavior in PA66 peaks. This time the values are naturally decreasing, but the decreasing is not linear with increasing GO content. This time the complex peak area values decrease faster when comparing blend with blend+GO1wt%. The decrease of the complex peak continues when comparing blend+GO1wt% with blend+GO2wt%, but the slope is clearly not as steep as with blend and blend+GO1wt% comparison. The results are presented in figure 19.

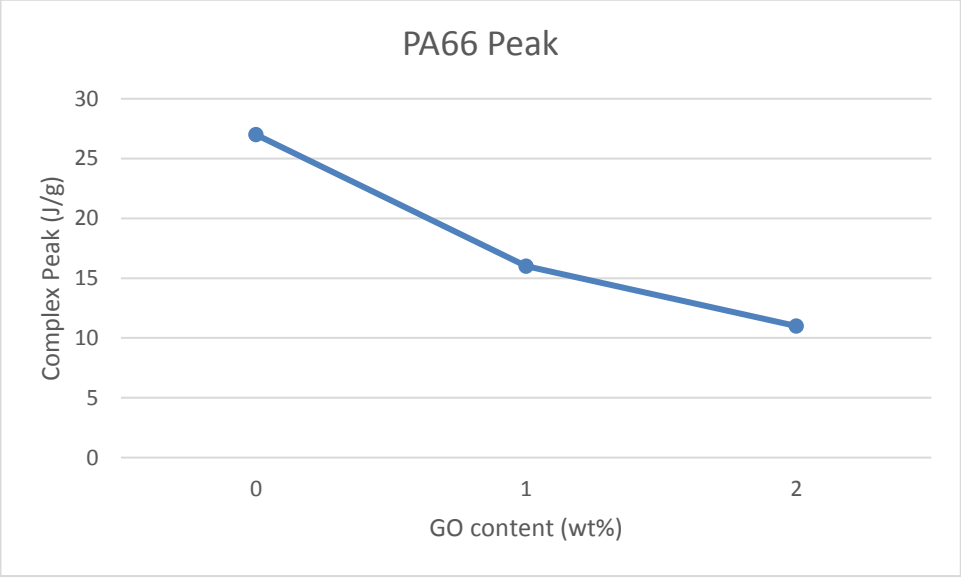

Figure 19. *Complex peak areas as a function of GO content in PA66 peak area.*

6.3.1 Degree of crystallinity

As seen from the DSC curves, the areas under melt peaks are changing in blend, blend+GO1wt% and blend+GO2wt%. This peak area is indicating melt enthalpy. Melt enthalpy can be then used to calculate the degree of crystallinity of the blends. The degree of crystallinity is determined by using the following equation.

$$K = \left(\frac{\Delta H_m}{\Delta H_{m^0}}\right) * 100\ [\%] \tag{4}$$

where, K is the degree of crystallinity, ΔH_m is experimental melting enthalpy and $\Delta H_m{}^0$ is a literature value for theoretical melting enthalpy.

Theoretical melting enthalpy of polyethylene has a literature value of 293 J/g and theoretical melting enthalpy of PA66 has a literature value of 226 J/g [49]. With these values, and the experimental melting enthalpy values from DSC results, degree of crystallinity can be calculated for the blends in both peaks.

LDPE Peaks:

$$K(Blend) = \left(\frac{70{,}06\frac{J}{g}}{293\frac{J}{g}}\right) * 100\ [\%] = 23.91\ \%$$

$$K(Blend + GO1wt\%) = \left(\frac{102{,}6\frac{J}{g}}{293\frac{J}{g}}\right) * 100\ [\%] = 35.02\ \%$$

$$K(Blend + GO2wt\%) = \left(\frac{114{,}2\frac{J}{g}}{293\frac{J}{g}}\right) * 100\ [\%] = 38.98\ \%$$

PA66 Peaks:

$$K(Blend) = \left(\frac{27{,}17\frac{J}{g}}{226\frac{J}{g}}\right) * 100\ [\%] = 12.02\ \%$$

$$K\ (Blend + GO1wt\%) = \left(\frac{15{,}75\frac{J}{g}}{226\frac{J}{g}}\right) * 100\ [\%] = 6.97\ \%$$

$$K\ (Blend + GO2wt\%) = \left(\frac{10{,}74\frac{J}{g}}{226\frac{J}{g}}\right) * 100\ [\%] = 4.75\ \%$$

The rounded-up values for crystallinity in blend, blend+GO1wt% and blend+GO2wt% are presented in table 5. The crystallinity values are presented in both peak areas.

Table 5. *Crystallinity values for blend, blend+GO1wt% and blend+GO2wt% in different peaks.*

Name	Peak	Crystallinity(%)
Blend	LDPE	24
Blend+GO1wt%		35
Blend+GO2wt%		39
Blend	PA66	12
Blend+GO1wt%		7
Blend+GO2wt%		5

The results show, that the crystallinity of the blends is rising in LDPE with increasing GO content. In the PA66, the crystallinity is decreasing with the increasing GO content. These results could indicate that GO is working as a compatibilizer and causing better PA66 dispersing in the LDPE matrix, since better dispersion would higher the crystallinity in the matrix polymer. This would then cause the higher energies needed to melt the LDPE because of better miscibility. That would also explain the decreasing crystallinity of PA66 peak with the addition of GO, since the PA66 amount dispersed in the matrix would be higher.

6.4 TGA results

Thermogravimetric analysis was performed to gain information about the structure of intercalating molecules by the weight loss steps. The TGA curves for blend, blend+GO1wt% and blend+GO2wt% are presented in figure 20. The figure also presents the onset temperatures for all the samples. The onset temperatures were determined by the TGA program, by extrapolating the tangents of the curves. Intersection of these tangents denotes the temperature where the weight loss begins in the samples.

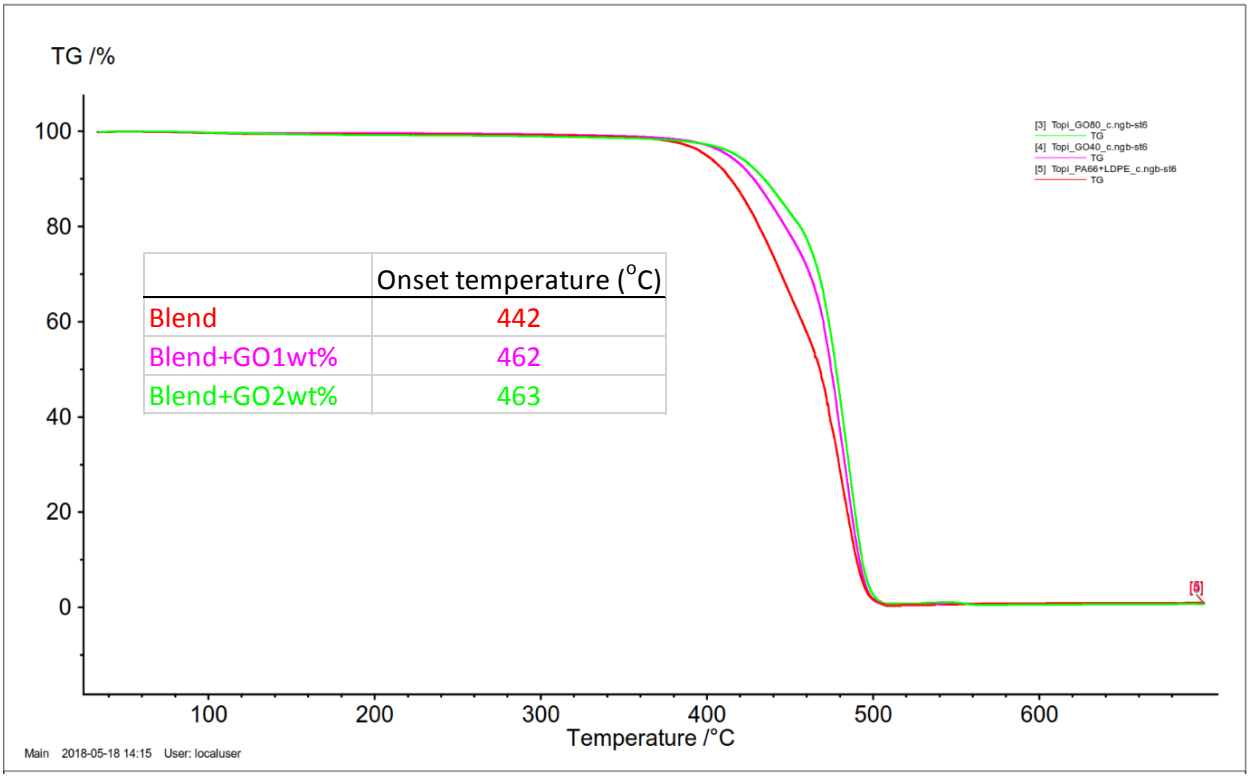

Figure 20. *TGA curves for blend, blend+GO1wt% and blend+GO2wt% and their onset temperatures.*

It can be seen from the TGA curves that a single degradation step happens in all the samples, suggesting that the addition of GO has not significantly changed the degradation mechanism for the polymers [50]. The addition of GO in the samples clearly increases the onset temperatures, which can be seen from figure 20. In the blend, the onset temperature is 442 °C. In the blend+GO1wt%, the onset temperature increases to 462 °C. In the blend+GO2wt%, the onset temperature is 463 °C. The addition of GO has a clear effect on the samples onset temperatures. This can be interpreted to delay the thermal degradation process, meaning better thermal stability of the samples with GO content in them. The thermal stability would be enhanced because of strong interactions between polymer(s) and GO, causing the degradation to slow down [51]. The difference between blend+GO1wt% and blend+GO2wt% onset temperatures is not large, so doubling the GO content does not seem to affect the onset temperatures much. The difference between the sample without GO and the samples with GO is, however, substantial.

6.5 FTIR results

FTIR was used to determine if GO interacted with the polymers, by studying the chemical structures in the samples. The results from the FTIR analysis are presented in figures 21, 22 and 23. In figure 21 the spectrums of blend, blend+GO1wt% and blend+GO2wt% are presented in 500 cm^{-1} – 4000 cm^{-1} area. All the figures also have LDPE spectrum. LDPE spectrum in figure 21 is used to present the characteristic groups, which are present in LDPE. Also, the LDPE spectrum is used as a comparison point to present the characteristic groups, which are related to PA66, in the other samples. The comparison between blend, blend+GO1wt% and blend+GO2wt% is presented in figures 22 and 23, where the shifting of the characteristic peaks is illustrated.

It can be seen in figure 21, that all the peaks which are visible in the LDPE spectrum are also visible in the spectrums of blend, blend+GO1wt% and blend+GO2wt%. This is no surprise, since all the samples have LDPE in them as well. Therefore, the spectrums of the samples should have the characteristic groups of both LDPE and PA66.

The peaks that occur between 2800 cm^{-1} and 3000 cm^{-1} are associated with simple C-H stretching vibrations. The higher valued peak in this area is related to C-H asymmetric stretching and the lower valued peak in this area is related to C-H symmetric stretching. The peak in under 1500 cm^{-1} area is associated with simple C-H bending vibrations. The peak in 720 cm^{-1} - 730 cm^{-1} area is associated with C-C rocking. All of these peaks are highlighted and named in the LDPE spectrum of figure 21. All these peaks are also characteristic peaks for polyethylene's [52].

In figure 21, the spectrums of blend, blend+GO1wt% and blend+GO2wt% also have some peaks in their spectrums that are not present in the LDPE spectrum. These peaks are related to the polyamide in the blends. Two peaks, which are characteristic for polyamides, are presented in figure 21. N-H bending peak, which is highlighted and marked in blend+GO1wt% spectrum and C=O stretching peak, which is highlighted and marked in blend spectrum [52].

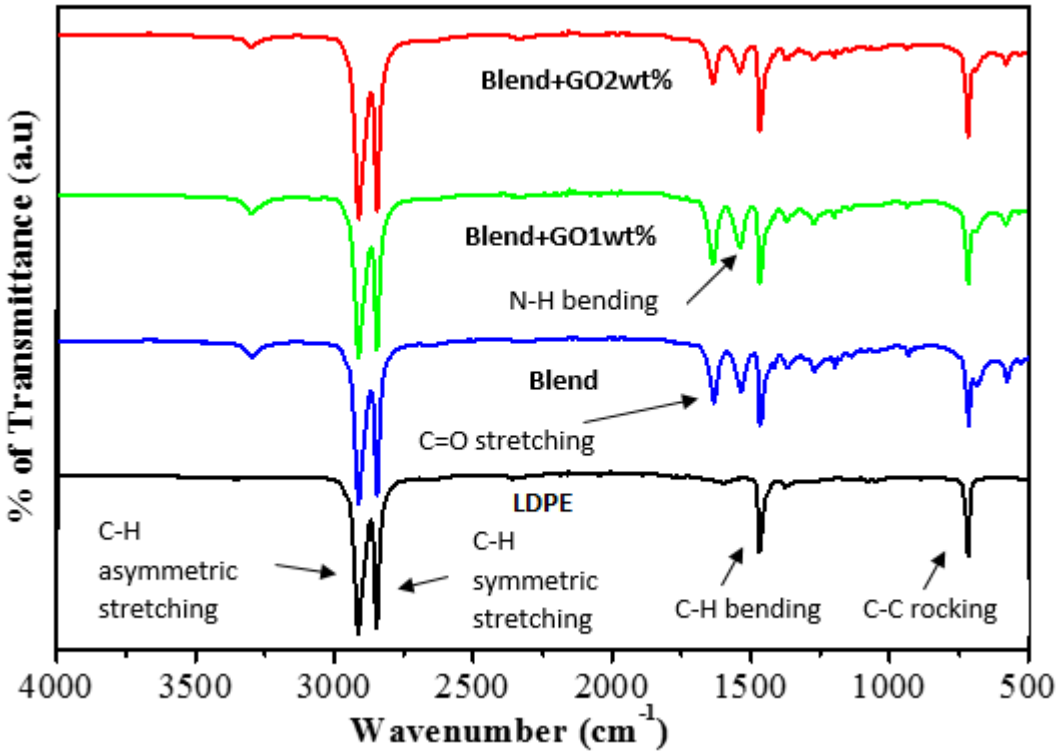

Figure 21. *FTIR spectrums for LDPE, blend, blend+GO1wt% and blend+GO2wt% in 500 cm^{-1} – 4000 cm^{-1} area.*

From the enlarged spectra in figure 22, it is easier to see that the peak positions are shifting in all the peak positions. To make the comparison more easily visible, the peak positions and their numeric values are marked in the spectra of LDPE, blend, blend+GO1wt% and blend+GO2wt%.

As presented in figure 22, the only peak visible in the LDPE spectrum is at 1470 cm^{-1}. The blend spectrum has a peak at this same position, but the peaks in the samples with GO content are shifting. Blend+GO1wt% spectrum has a peak at 1468 cm^{-1} and blend+GO2wt% has a peak at 1467 cm^{-1}. These peaks are associated with C-H bending vibration, which is a characteristic group in polyethylene [52].

Figure 22 also presents peaks which are characteristic for polyamides. The peaks at 1537 cm^{-1} in the blend spectrum, 1540 cm^{-1} in the blend+GO1wt% spectrum and 1541 cm^{-1} in the blend+GO2wt% spectrum, are all associated with N-H bending vibration. And as it can be seen from the values, the peak is slightly shifting. The other peaks occur at 1632 cm^{-1} in the blend spectrum, 1636 cm^{-1} in the blend+GO1wt% spectrum and 1637 cm^{-1} in the blend+GO2wt% spectrum. These peaks are associated with C=O stretching vibration and shifting is once again witnessed [52].

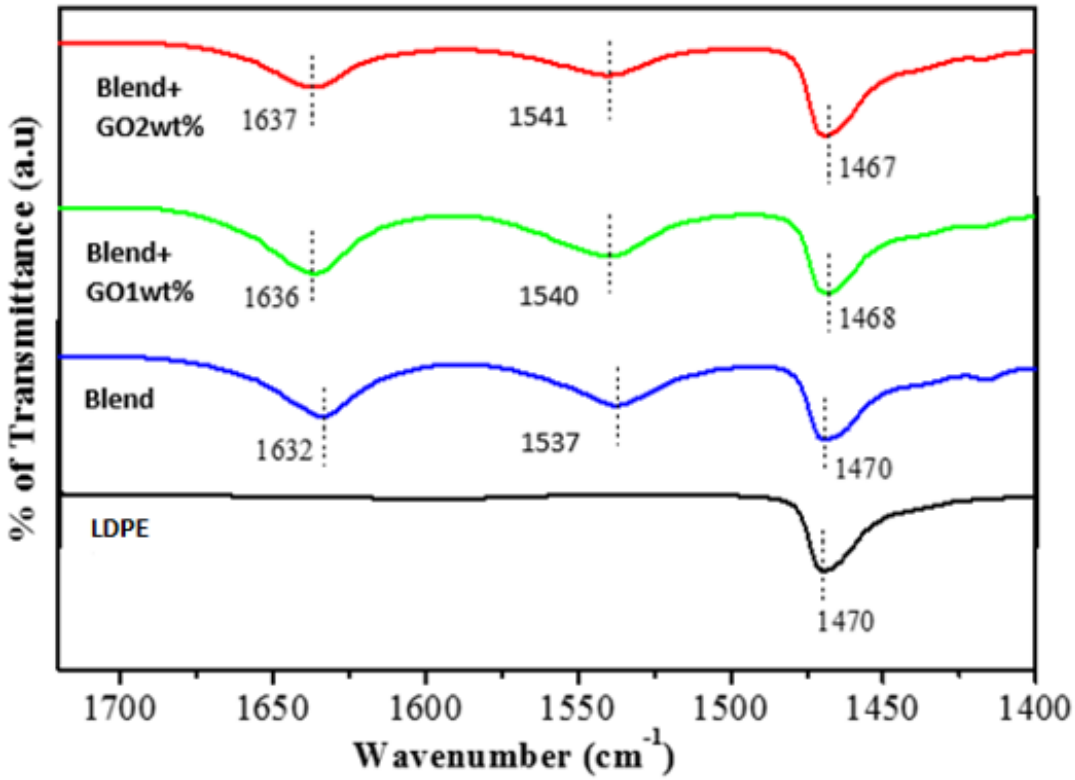

Figure 22. *FTIR spectrums for LDPE, blend, blend+GO1wt% and blend+GO2wt% in enlarged 1400 cm^{-1} – 1750 cm^{-1} area.*

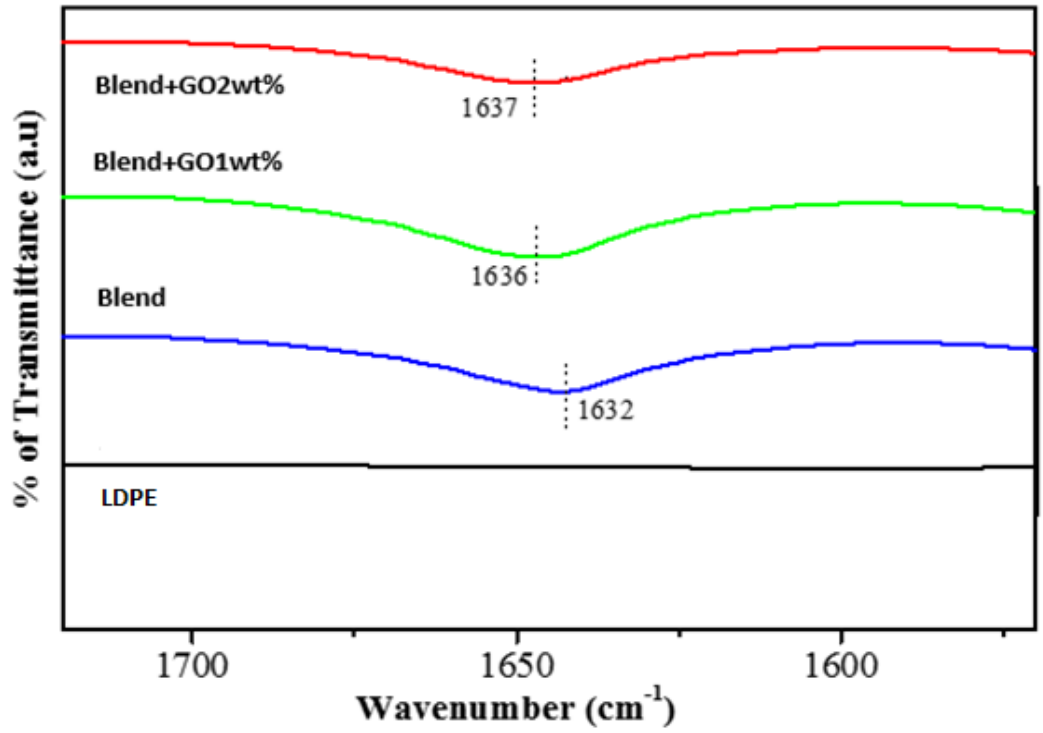

Figure 23. *FTIR spectrums for LDPE, blend, blend+GO1wt% and blend+GO2wt% with the shifting of C=O stretching vibration peak.*

In figure 23, the shifting of C=O stretching vibration peaks are enlarged even more. This time the spectra of LDPE, blend, blend+GO1wt% and blend+GO2wt% are presented at the area of 1550 cm^{-1} – 1750 cm^{-1}. With this enlarged figure, the shifting of the peaks is seen even more clearly.

In figures 22 and 23, the shifting of different characteristic peaks is illustrated. The shifting is happening to higher wave numbers in the characteristic groups related to PA66. On the other hand, the shifting is happening to lower wave numbers in the characteristic group related to LDPE. These slight shifts indicate that GO is interacting with different groups, especially with the amine group of PA66 via hydrogen bonding [53]. Same kind of shifting has been reported by other studies with GO and polyamide as well [54].

The bonding with PA66 and GO is a good thing, because interactions between the polymers and GO is an important aspect of compatibilization [53]. The characteristic vibrations and the shifting for the different spectra are presented in table 6.

Table 6. *Characteristic groups and their peak values in FTIR spectrums for LDPE, blend, blend+GO1wt% and blend+GO2wt%.*

Characteristic group	LDPE (cm^{-1})	Blend (cm^{-1})	Blend+GO1wt% (cm^{-1})	Blend+GO2wt% (cm^{-1})
C-H Bending vibration	1470	1470	1468	1467
N-H Bending vibration		1537	1540	1541
C=O Stretching vibration		1632	1636	1637

6.6 Chemical interactions

Graphite has many useful properties, but it also has a high chemical inertia. This causes graphite to have low compatibility with many materials [55]. GO, on the other hand, easily disperses into polymer matrices because of its hydrophilic nature. Another good property of GO is, that it contains aliphatic and aromatic domains. Therefore, there are many possibilities for different interactions to happen on the surface [40].

Polyolefins, like LDPE in this work, can interact with graphene structures via CH-π interactions [56]. These non-covalent interactions are weak by themselves. The strength of CH-π interaction is only one tenth of the strength of hydrogen bond [43]. However, if enough CH-linkages are present, then CH-π interactions can cooperatively have impact on many chemical phenomena, like forming molecular complexes [40,43]. These kinds of non-covalent interactions also have another important property. The non-covalent interactions do not interrupt the extended π conjugation of the graphenic nanostructures, which has an important role on maintaining many of the properties [40].

The amide groups (-CONH-) in PA66 can form a hydrogen bond with the functional groups of graphene [53]. In this work the amide groups form hydrogen bonding with carboxyl and hydroxyl groups. The presence of these bonds can be evidenced from the FTIR spectra.

The CH-π interactions and the hydrogen bonding are also functionalizing the GO. This is called non-covalent functionalization of graphene with polymers [40,42]. The high shear forces in the melt blending process also help in functionalization [42]. As the melt blending was done at the temperature of 270 ºC it has also affected the functional groups of GO. Because of the thermal processing, most of the functional groups of GO are most likely decomposed from the structure [37,38]. Therefore, the material can be called partially thermally reduced GO.

With the theoretical information and the results from analyzing methods, a figure with the polymers and partially reduced GO is illustrated. Hydrogen bonding and CH-π interactions of the LDPE-rGO-PA66 system are presented in figure 24.

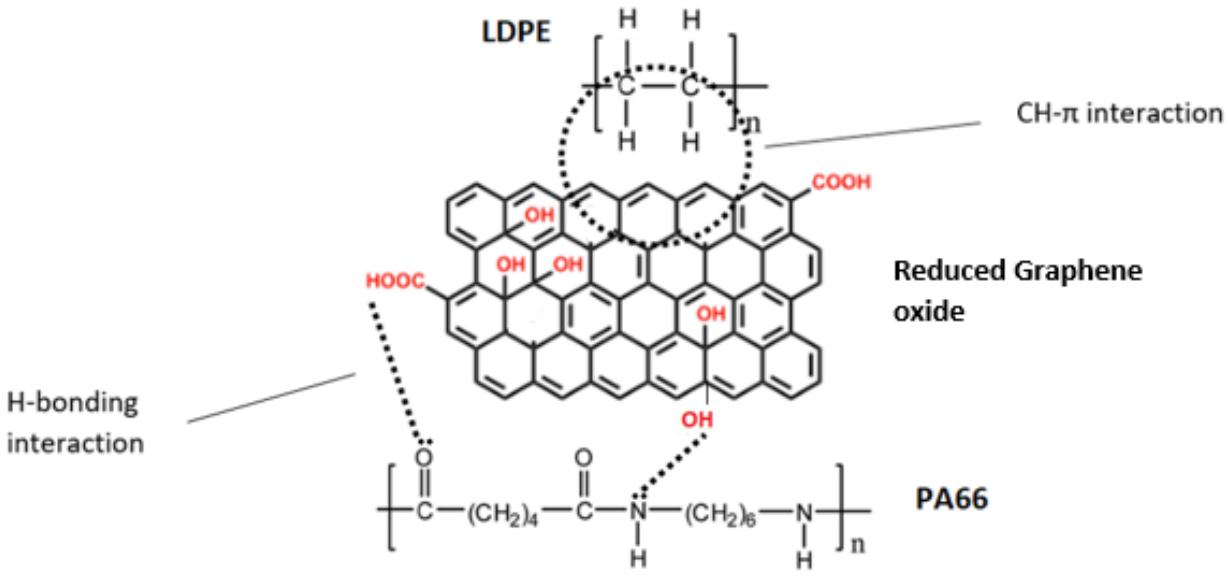

Figure 24. *CH-π interactions between partially reduced GO and LDPE. H-bonding interactions between the functional groups of partially reduced GO and the amide group of PA66.*

Figure 24 illustrates the chemical structures of LDPE and PA66. LDPE's structure contains carbon and hydrogen atoms bonded together. PA66 has carbon and hydrogen atoms and the amide group (-CONH-). The structure of rGO is also illustrated with the functional groups of carboxyl and hydroxyl present.

As presented in figure 24, the partially reduced GO is forming bonds with LDPE matrix and the PA66 component. The CH-π interactions are illustrated by circle formed by dashed line. The CH-bonds are in the LDPE structure, and the π-bond domains are in the structure of partially reduced GO, which is inside the circle. The hydrogen bonds formed between the amide group of PA66 and the carboxyl and hydroxyl groups of partially reduced GO are presented with two dashed lines.

6.7 Further research

This research proved to have some nice results from different analyzing methods. As the research of graphene working as a compatibilizer is still in fairly early stages, other methods could still be exploited to gather further information about the properties of the manufactured blends.

Information about mechanical properties would be one thing for a further research. Tensile testing could be the method to be exploited in mechanical testing. In this way, more information about the possibly enhanced mechanical properties could be gathered.

Also, gas barrier testing of the different films would provide valuable information about the blends' properties. With the two polymers in this thesis, PA66 should improve the gas barrier properties of the blend. The barrier properties are an important property of different film applications in packaging industry.

During this thesis, I also did some research on other possible materials to be used in this kind of blending. The most interesting material seemed to be PA6. Several different grades of PA6 are available that would have the necessary properties to perform same kind of research as was done during this thesis. The biggest advantage of those grades compared to the PA66 used in this work is, that their processing temperatures are significantly lower. The processing and melting temperatures are much closer to the LDPE which would, for example, make the processing easier.

If the results continue to be encouraging, then there is no reason not to take the research into a bigger scale. Bigger extruders could be exploited in some point of the research to see if the laboratory scale research results correlate with results from industrial scale extruders. This would also provide information about what kind of extruders are capable of mixing GO with polymers. Especially information on single-screw extruder designs mixing capability of GO and polymers would provide valuable information.

7. CONCLUSIONS

Polymer blending can provide an efficient way to create materials with enhanced properties. Different chemical structure of the blends components usually causes phase separation and causes the blend to be immiscible, which affect the properties of the blend in a negative way. The interface properties of immiscible blends can be enhanced by adding a compatibilizer, which then stabilizes the morphology, lowers the interfacial tension and enhances finer dispersion.

Graphene and other materials which are based on graphene have numerous unique properties, including large surface area and good chemical properties. This has caused interest in graphenic materials, since because of their properties, they could potentially be exploited in many applications. Graphene oxide (GO), which can be created with synthesis from graphite, has interesting properties like easy dispersibility into polymer matrices, which could lead to its potential use as a compatibilizer. By functionalizing graphene or GO, the best possible properties of those materials can be exploited, and these materials can be, for example, combined with other materials.

During this thesis, blends were created by melt compounding to assess if GO enhances the properties of the blends. Melt compounding was done by using a laboratory scale intermeshing corotating twin-screw extruder. The polymer materials in the blends were low-density polyethylene (LDPE) as matrix and polyamide66 (PA66) as second component. The highly immiscible polymers were compatibilized by GO, which was added into the extruder by the use of masterbatches. Masterbatches were created by exploiting GO's dispersibility in organic solvents, like acetone used in this work.

GO was produced by modified Hummers' method. GO was partially reduced with the high temperatures in the melt compounding process. GO was also functionalized to exploit its properties. The functionalization of GO was done by non-covalent method, exploiting π interactions and hydrogen bonding. High shear forces in the melt processing with the twin-screw extruder enhance these non-covalent interactions.

Several analyzing methods were performed for the processed samples to collect data and to compare the samples. Analyzing methods included FESEM, XRD, DSC, TGA and FTIR. The results from analyzing methods were evaluated in terms of properties and changes in them with the addition of GO.

FESEM images from different samples show a drastic change in hole sizes, which were created by etching the samples. The holes in the samples with GO in them show much more uniform dispersion and smaller hole sizes than the samples without GO. The addition of GO clearly improves dispersion of PA66 in LDPE matrix.

XRD was used first to confirm, that the modified Hummers' method had produced good quality GO. This is evidenced from the diffraction peak indicating that the oxygen functionalized groups are present at the structure of GO. The absence of this peak in the blends also suggest the uniform dispersion of GO in the polymer matrices.

Crystallinity of LDPE is enhancing according to DSC results. This is also in line with other results, as it would suggest that PA66 is dispersed into the matrix. The lowering crystallinity values at the PA66 peak are also supporting this.

TGA analysis shows significantly improved thermal stability with the blends formed with GO in them. The difference of the onset temperatures between the two GO blends is low. This indicates that thermal stability increases with GO but does not increase with the same rate as GO content is getting higher in blends.

FTIR spectroscopy provides information about the chemical structures and chemical changes in the samples. Comparison of spectra is done, and the results are promising. Shifting of different peaks occur in different areas. The most interesting shifts occur in area of different characteristic groups of polyamides. The shifts in N-H bending vibration area and C=O stretching area occur in both blends with GO in them. These slight shifts are indicating that the polar functional groups of PA66 area bonding with the functional oxygen containing groups in the structure of GO via hydrogen bonding.

Overall, blending process of the polymers and GO seem to have succeeded. With strong theoretical background supporting the thesis and by exploiting many analyzing methods, good indications of compatibilization of immiscible blends with GO are witnessed. The results from different analyzing methods indicate enhanced dispersion of PA66 in LDPE matrix. Good dispersion is one of the key things in enhancing interfacial properties and therefore producing blend with desirable properties. Also encouraging signs of chemical bonding is witnessed from FTIR spectra.

REFERENCES

[1] E. S. Pino, M. A. F. Feitosa, Mechanical properties of polyamide 6,6 / low-density polyethylene blend by ionizing radiation, International Nuclear Atlantic Conference, Brazil, 2007, 4p. Available: https://www.ipen.br/biblioteca/cd/inac/2007/pdf_dvd/E13_1318.pdf

[2] A.B. Strong, Plastics: Materials and Processing, Third Edition, Pearson Education Inc, USA, 2006, 917p.

[3] L. Elias, F. Fenouillot, J. C. Majeste, Ph. Cassagnau, Morphology and rheology of immiscible polymer blends Filled with silica nanoparticles, Congres Francais du Mecanique, France, 2009.

[4] S. C. Ray, Applications of Graphene and Graphene-Oxide Based Nanomaterials, Elsevier, UK, 2015, pp. 39-53.

[5] S. Pei, H.-M. Cheng, Reduction of Graphene oxide, Carbon, Vol. 50, Issue 9, 2012, pp. 3210-3228.

[6] J. Lahti, Polymeric Materials: Thermoplastics Part 1, Tampere University of Technology, Tampere, Finland, 2016.

[7] M. Kolev, Polyethylene(polyethene)(PE), Technical University of Gabrovo, Gabrovo, Bulgaria, 2008. 9p. Available in finnish: http://www.valuatlas.fi/tietomat/docs/plastics_PE_FI.pdf

[8] L. H. Sperling, Introduction to Physical Polymer Science, Fourth Edition, Wiley-Interscience, USA, 2005, 845 p.

[9] C. Vasile, M. Pascu, Practical guide to polyethylene, Rapra Publishing, UK, 2005, 188p.

[10] T. I. Butler, Low-Density Polyethylene, Blown Film Tech, USA, 18p. Available: http://blownfilmtech.com/eBooks/Free/LDPE.pdf

[11] M. A. Spalding, A. M. Chatterjee, Handbook of Industrial Polyethylene and Technology: Definitive Guide to Manufacturing, Properties, Processing, Applications and Markets, First Edition, John Wiley & Sons, Scrivener Publishing, USA, 2017, 1410p.

[12] Essential Chemical Industry, Poly(ethene) (Polyethylene), 2007. Available: http://www.essentialchemicalindustry.org/polymers/polyethene.html

[13] W. Goetz, Polyamide for Flexible Packaging film, PLACE Conference, Italy, 2003, 57p. Available: http://www.tappi.org/content/enewsletters/eplace/2004/10-2goetz.pdf

[14] I. B. Page, Polyamides as Engineering Thermoplastic Materials, iSmithers Rapra Publishing, United Kingdom, 2000, pp. 2-24.

[15] J. A. Brydson, Edited by M. Gilbert, Brydson's Plastic Materials, Eight Edition, Elsevier Ltd, 2017, pp. 487-510.

[16] B. A. Ibrahim, K. M. Kadum, Influence of Polymer Blending on Mechanical and Thermal Properties, Canadian Center of Science and Education, Modern Applied Science, Vol. 4, No. 9, Canada, 2010, pp. 157-161.

[17] Y. Cao, J. Zhang, J. Feng, P. Wu, Compatibilization of Immiscible Polymer Blends Using Graphene Oxide Sheets, American Chemical Society, USA, 2011. Available:https://pubs.acs.org/doi/suppl/10.1021/nn201717a/suppl_file/nn201717a_si_001.pdf

[18] H. Wang, Z. Fu, W. Dong, Y. Li, J. Li, Formation of Interfacial Janus Nanomicelles by Reactive Blending and Their Compatibilization Effects on Immiscible Polymer Blends, American Chemical Society, Journal of Physical Chemistry, 2016, pp. 9240-9252 Available: https://pubs.acs.org/doi/suppl/10.1021/acs.jpcb.6b06761/suppl_file/jp6b06761_si_001.pdf

[19] J.-P. Qu, H.-Z. Chen, S.-R. Liu, B. Tan, L.-M. Liu, X.-C. Yin, Q.-J. Liu, R.-B. Quo, Morphology Study of Immiscible Polymer Blends in a Vane Extruder, Wiley, Journal of Applied Polymer Science, Vol. 128, Issue 6, 2012, pp. 3576-3585.

[20] V. Khoshkava, M. Dini, H. Nazockdast, Study on Morphology and Microstructure Development of PA6/LDPE/Organoclay Nanocomposites, Journal of Applied Polymer Science, Vol. 125, Wiley, 2011, pp. 197-203.

[21] P. Xavier, P. Rao, S. Bose, Nanoparticle induced miscibility in LCST polymer blends: critically assessing the enthalpic and entropic effect, Royal Society of Chemistry, Physical Chemistry Chemical Physics, Issue 1, 2016, pp. 47-64. Available: http://pubs.rsc.org/en/content/articlehtml/2016/cp/c5cp05852j

[22] L. A. Utracki, C. Wilkie, Polymer Blends Handbook, Second Edition, Springer, Netherlands, 2014, pp. 172-254.

[23] S. Ebnesajjad, Plastic Films in Food Packaging: Materials, Technology and Applications, USA, 2013, pp. 317-333.

[24] L. M. Robeson, Polymer Blends: A Comprehensive Review, Hanser, Germany, 2007, pp. 11-23.

[25] M. Salzano de Luna, G. Filippone, Effects of nanoparticles on the morphology of immiscible polymer blends – Challenges and opportunities, European Polymer Journal 79, Elsevier, 2016, pp. 198-218. Available: https://www.sciencedirect.com/science/article/pii/S0014305716300805

[26] C. I. Chung, Extrusion of Polymers: Theory & Practise, Second Edition, Hanser, Germany, 2011, pp. 13-56.

[27] T. A. Osswald, G. Menges, Materials Science of Polymers for Engineers, Second Edition, Hanser, Germany, 2003, 622p.

[28] I. Jönkkäri, Extrusion: Single-screw extrusion, Tampere University of Technology, Tampere, Finland, 2017.

[29] C. Martin, In the Mix: Continuous Compounding Using Twin-Screw Extruders, Medical Device & Diagnostic Industry Magazine, 2000. Available: https://www.mddionline.com/mix-continuous-compounding-using-twin-screw-extruders

[30] M. H. N. Famili, S. Morandi, A Fast and Economical Method for Producing of Self-wipe Twin-screw Extruder Modules, The Open Mechanical Engineering Journal, Iran, 2008, pp. 93-96. Available: https://pdfs.semanticscholar.org/9909/33e44811cbde7ad234818a7a7ddf986d8a29.pdf

[31] J.-N. Fuchs, M. O. Goerbig, Introduction to the Physical Properties of Graphene, Lecture Notes, 2008. Available: http://web.physics.ucsb.edu/~phys123B/w2015/pdf_CoursGraphene2008.pdf

[32] E. Jimenez-Cervantes Amieva, J. Lopez-Barroso, A. L. Martinez.Hernandes, C. Velasco-Santos, Graphene-Based Materials Functionalization with Natural Polymeric Biomolecules, Recent Advantages in Graphene Research, InTech, 2016, pp. 257-298. Available: https://cdn.intechopen.com/pdfs/51598.pdf

[33] A. Ammar, A. M. Al-Enizi, M. AlAli AlMadeed, A. Karim, Influences of graphene oxide on mechanical, morphological, barrier, and electrical properties of polymer membranes, Arabian Journal of Chemistry, 2015.

[34] S. Pei, H.-M. Cheng, Reduction of Graphene oxide, Carbon, Vol. 50, Issue 9, 2012, pp. 3210-3228.

[35] Q. Zheng, J.-K. Kim, Graphene for Transparent Conductors, Springer, USA, 2015, pp. 29-94.

[36] X. Zhang, Graphene-Based Functional Materials, Ph.D. Thesis, Netherlands, 2013, 170 p.

[37] O. M. Slobodian, P. M. Lytvyn, A. S. Nikolenko, V. M. Naseka, O. Y. Khyzhun, A. V. Vasin, S. V. Sevostianov, A. N. Nazarov, Low-Temperatrue Reduction of Graphene Oxide: Electrical Conductance and Scanning Kelvin Probe Force Microscopy, Springer, Nanoscale Research Letters, 2018. Available: https://www.researchgate.net/publication/325028143_Low-Temperature_Reduction_of_Graphene_Oxide_Electrical_Conductance_and_Scanning_Kelvin_Probe_Force_Microscopy

[38] W. Chen, L. Yan, Preparation of graphene by a low-temperature thermal reduction at atmosphere pressure, The Royal Society of Chemistry, Nanoscale, 2010, pp. 559-563.

[39] R. K. Singh, R. Kumar, D. P. Singh, Graphene oxide: strategies for synthesis, reduction and frontier applications, The Royal Society of Chemistry, RSC Advances, Issue 6, 2016, pp. 64993-65011.

[40] V. Georgakilas, J. N. Tiwari, K. C. Kemp, J. A. Perman, A. B. Bourlinos, K. S. Kim, R. Zboril, Noncovalent Functionalization of Graphene and Graphene Oxide for Energy Materials, Biosensing, Catalytic, and Biomedical Applications, American Chemical Society, Chemical Reviews, 2016, pp. 5464-5519. Available: https://pubs.acs.org/doi/pdf/10.1021/acs.chemrev.5b00620

[41] R. K. Layek, A. K. Nandi, A review on synthesis and properties of polymer functionalized graphene, Elsevier Ltd., Polymer, Vol. 54, Issue 19, 2013, pp. 5087-5103. Available: https://ac.els-cdn.com/S0032386113005636/1-s2.0-S0032386113005636-main.pdf?_tid=d15c001e-f610-442c-a6b9-8b90e1002db3&acdnat=1530889031_5797caf5062bba2c6174f994e2e48be8

[42] W. Zheng, B. Shen, W. Zhai, Surface Functionalization of Graphene with Polymers for Enhanced Properties, InTech, New Progress on Graphene Research, 2013, pp. 207-234. Available: http://cdn.intechopen.com/pdfs/37771/InTech-Surface_functionalization_of_graphene_with_polymers_for_enhanced_properties.pdf

[43] V. K. Thakur, M. K. Thakur, Chemical Functionalization of Carbon Nanomaterials: Chemistry and Applications, CRC Press, USA, 2015, pp. 833-837.

[44] S. N. Tripathi, G. S. Srinivasa Rao, A. B. Mathur, R. Jasra, Polyolefin/graphene nanocomposites: a review, Royal Society of Chemistry, vol. 7, 2017, pp. 23615-23632. Available: http://pubs.rsc.org/en/content/articlehtml/2017/RA/C6RA28392F

[45] S. Thomas, R. Muller, J. Abraham, Rheology and Processing of Polymer Nanocomposites, John Wiley & Sons, USA, 2016, pp. 29-61.

[46] C. Fu, G. Zhao, H. Zhang, S. Li, Evaluation and Characterization of Reduced Graphene Oxide Nanosheets as Anode Materials for Lithium-Ion Batteries, International Journal of Electrochemical Science, 2013, pp. 6269-6280. Available: http://www.electrochemsci.org/papers/vol8/80506269.pdf

[47] I. B. Inuwa, A. Hazzan, S. A. Samsudin, M. H. M. Kassim, M. Jawaid, Mechanical and Thermal Properties Exfoliated Graphite Nanoplatelets Reinforced Polyethylene Terephthalate/Polypropylene Composites, Wiley, Polymer Composites, Vol. 35, Issue 10, 2014, pp. 2029-2035.

[48] S. Vyazovkin, N. Koga, C. Schick, Hanbook of Thermal Analysis and Calorimetry: Recent Advances, Techniques and Applications, Second Edition, Vol. 6, Elsevier, Netherlands, 2018, pp. 70-75.

[49] R. L. Blaine, Thermal Applications Note: Polymer Heats of Fusion, TA Instruments, USA. Available: http://www.tainstruments.com/pdf/literature/TN048.pdf

[50] B. Qi, Z. Yuan, S. Lu, K. Liu, S. Li, L. Yang, J. Yu, Mechanical and Thermal Properties of Epoxy Composites Containing Graphene Oxide and Liquid Crystalline Epoxy, Korean Fiber Society, Springer, Fibers and Polymers, Vol. 15, No. 2, 2014, pp. 326-333. Available: https://www.researchgate.net/publication/271742373_Mechanical_and_Thermal_Properties_of_Epoxy_Composites_Containing_Graphene_Oxide_and_Liquid_Crystalline_Epoxy?_sg=YIJ4OQILjCayLAAghXJe8f1YsufPxw5-7Z4lE4cTqv-4Gy9zhJPF7_yRr32aP2f2JLcfxSGPYg

[51] A. S. Luyt, Using thermogravimetric analysis to determine polymer thermal stability: Relevance of changes in onset temperature of mass loss, eXPRESS Polymer Letters, Vol. 9, No. 9, 2015.

[52] J. Coates, Interpretation of Infrared Spectra, A Practical Approach, Encyclopedia of Analytical Chemistry, John Wiley & Sons Ltd, United Kingdom, 2000, pp. 10815-10837.

[53] W. S. Chow, Z. A. Mohd Ishak, Polyamide blend-based nanocomposites: A review, eXPRESS Polymer Letters, Vol. 9, No. 3, 2015, pp. 211-232.

[54] T. Y. Hui, Development of Nylon-6/Graphene oxide (GO) High Performance Nanocomposites, B.Sc. Thesis, 2015.

[55] L. Alexandrescu, M. Sönmez, M. Georgescu, M. Nituica, A. Ficai, R. Trusca, D. Gurau, L. Tudoroiu, Polyamide/polypropylene/graphene oxide nanocomposites with functional compatibilizers: Morpho-structural and physico-mechanical characterization, Elsevier, Procedia Structural Integrity, Vol. 5, 2017, pp. 675-682. Available: https://reader.elsevier.com/reader/sd/75CE51C1929F90F68A8B7ABFCB96E124D7195CC01635D64BBFE563A0E7B48EF3F1543E196326D501AD354739564D2B84

[56] G. Carotenuto, S. De Nicola, G. Ausanio, D. Massarotti, L. Nicolais, G. Piero Pepe, Synthesis and characterization of electrically conductive polyethylene-supported graphene films, Springer, Nanoscale Research Letters, 2014. Available: https://www.ncbi.nlm.nih.gov/pmc/articles/PMC4184169/pdf/1556-276X-9-475.pdf